

AD-A125 248

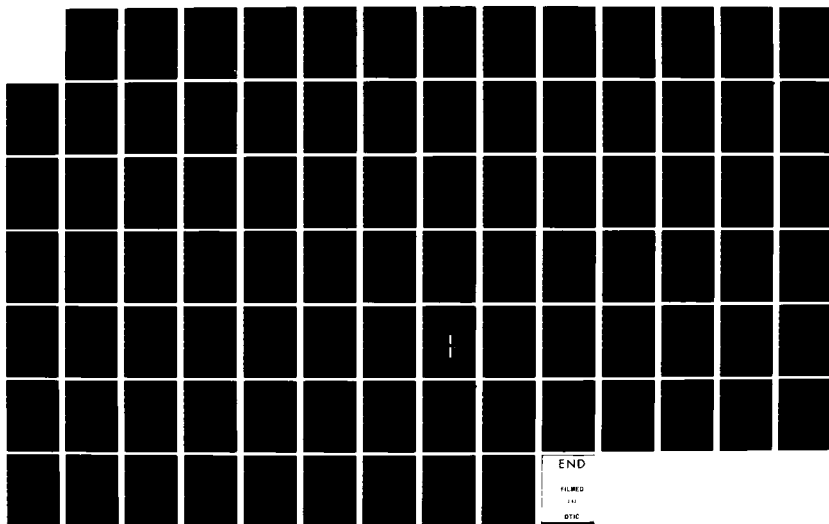
MATHEMATICAL MODELING OF BLACK-AND-WHITE CHROMOGENIC
IMAGE STABILITY(U) AIR FORCE INST OF TECH
WRIGHT-PATTERSON AFB OH C P DATEMA OCT 82
AFIT/CI/NR-82-66T

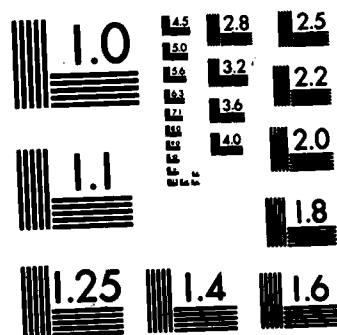
1/1

UNCLASSIFIED

F/G 14/5

NL





MICROCOPY RESOLUTION TEST CHART
NATIONAL BUREAU OF STANDARDS-1963-A

SECURI

AD A125248

READ INSTRUCTIONS
BEFORE COMPLETING FORM

1. REF

AFIT/CI/NR 82-66T

SION NO.

3. RECIPIENT'S CATALOG NUMBER

4. TITLE (and Subtitle)

Mathematical Modeling of Black-and-White
Chromogenic Image Stability

5. TYPE OF REPORT & PERIOD COVERED

THESIS/DISSERTATION

6. PERFORMING ORG. REPORT NUMBER

7. AUTHOR(s)

Charles Philip Datema

8. CONTRACT OR GRANT NUMBER(s)

9. PERFORMING ORGANIZATION NAME AND ADDRESS

AFIT STUDENT AT: Rochester Institute of
Technology10. PROGRAM ELEMENT, PROJECT, TASK
AREA & WORK UNIT NUMBERS

11. CONTROLLING OFFICE NAME AND ADDRESS

AFIT/NR
WPAFB OH 45433

12. REPORT DATE

Oct 82

13. NUMBER OF PAGES

76

14. MONITORING AGENCY NAME & ADDRESS (if different from Controlling Office)

15. SECURITY CLASS. (of this report)

UNCLASS

15a. DECLASSIFICATION/DOWNGRADING
SCHEDULE

16. DISTRIBUTION STATEMENT (of this Report)

APPROVED FOR PUBLIC RELEASE; DISTRIBUTION UNLIMITED

17. DISTRIBUTION STATEMENT (of the abstract entered in Block 20, if different from Report)

18. SUPPLEMENTARY NOTES

APPROVED FOR PUBLIC RELEASE: IAW AFR 190-17

LYNN E. WOLAVER

Dean for Research and

Professional Development

AFIT, Wright-Patterson AFB OH

19. KEY WORDS (Continue on reverse side if necessary and identify by block number)

20. ABSTRACT (Continue on reverse side if necessary and identify by block number)

ATTACHED

DTIC
SELECTED
MAR 4 1983
A

DD FORM 1 JAN 73 1473

EDITION OF 1 NOV 65 IS OBSOLETE

UNCLASS

SECURITY CLASSIFICATION OF THIS PAGE (When Data Entered)

88 03 03 041



Accession For	
NTIS GRA&I	<input checked="checked" type="checkbox"/>
DTIC TAB	<input type="checkbox"/>
Unannounced	<input type="checkbox"/>
Justification	
By	
Distribution/	
Availability Codes	
Dist	Avail and/or Special
A	

MATHEMATICAL MODELING OF
BLACK-AND-WHITE CHROMOGENIC IMAGE STABILITY

by

Charles Philip Datema

Submitted to the Photographic Science and
Instrumentation Division in partial fulfillment
of the requirements for the Master of Science
degree at the Rochester Institute of Technology

ABSTRACT

Agfapan Vario-XL film was faded at various levels of temperature, humidity, light, and fade time to determine the mathematical relationships of these variables and to examine whether interaction occurs between each factor. Light stability of the film was measured, and the Arrhenius relationship was used to predict dark stability at ambient storage conditions.

It was found that the amount of fade, as measured as either a change in transmittance or density, could be mathematically modeled with a high degree of correlation. Each independent variable (temperature, humidity, and time) was interactive with the other two variables.

DTIC
ELECTE
MAR 4 1983
A

Under the specific conditions tested, a significant interaction existed between light and dark fading reactions. For example, both the light and dark cyan dye reactions inhibit each other. However, in the case of the magenta and yellow dyes, a synergistic, or catalytic, effect occurs when light fading precedes dark fading.

Agfapan Vario-XL is extremely light stable when irradiated by a conventional enlarger light source.) An intermittency effect was noted. The dark stability compares with some of the least stable chromogenic print films - - a ^{10%}~~ten percent~~ loss in printing density is predicted by Arrhenius extrapolation when the Agfapan Vario-XL is stored at room temperature at 45 [%]~~percent~~ relative humidity for five years.

AFIT RESEARCH ASSESSMENT

The purpose of this questionnaire is to ascertain the value and/or contribution of research accomplished by students or faculty of the Air Force Institute of Technology (ATC). It would be greatly appreciated if you would complete the following questionnaire and return it to:

AFIT/NR
Wright-Patterson AFB OH 45433

RESEARCH TITLE: Mathematical Modeling of Black-and-White Chromogenic Image Stability

AUTHOR: Charles Philip Datema

RESEARCH ASSESSMENT QUESTIONS:

1. Did this research contribute to a current Air Force project?
☐ a. YES ☐ b. NO
2. Do you believe this research topic is significant enough that it would have been researched (or contracted) by your organization or another agency if AFIT had not?
☐ a. YES ☐ b. NO
3. The benefits of AFIT research can often be expressed by the equivalent value that your agency achieved/received by virtue of AFIT performing the research. Can you estimate what this research would have cost if it had been accomplished under contract or if it had been done in-house in terms of manpower and/or dollars?
☐ a. MAN-YEARS ☐ b. \$
4. Often it is not possible to attach equivalent dollar values to research, although the results of the research may, in fact, be important. Whether or not you were able to establish an equivalent value for this research (3. above), what is your estimate of its significance?
☐ a. HIGHLY SIGNIFICANT ☐ b. SIGNIFICANT ☐ c. SLIGHTLY SIGNIFICANT ☐ d. OF NO SIGNIFICANCE
5. AFIT welcomes any further comments you may have on the above questions, or any additional details concerning the current application, future potential, or other value of this research. Please use the bottom part of this questionnaire for your statement(s).

NAME

GRADE

POSITION

ORGANIZATION

LOCATION

STATEMENT(s):

82-66

MATHEMATICAL MODELING OF
BLACK-AND-WHITE CHROMOGENIC IMAGE STABILITY

by

Charles Philip Datema
B.S. Bob Jones University
(1968)

A thesis submitted in partial fulfillment
of the requirements for the degree of
Master of Science in the School of
Photographic Arts and Sciences in the
College of Graphic Arts and Photography
of the Rochester Institute of Technology

October, 1982

Signature of the Author


Photographic Science
and Instrumentation

Accepted by


Coordinator, Graduate Program

**MATHEMATICAL MODELING OF
BLACK-AND-WHITE CHROMOGENIC IMAGE STABILITY**

CHARLES PHILIP DATEMA

October, 1982

School of Photographic Arts and Sciences
Rochester Institute of Technology
Rochester, New York

CERTIFICATE OF APPROVAL

MASTER'S THESIS

The Master's Thesis of Charles P. Datema
has been examined and approved
by the thesis committee as satisfactory
for the thesis requirement for the
Master of Science degree

Milton Pearson
.....
Mr. Milton Pearson, Thesis Advisor

James M. Reilly
.....
Mr. James Reilly

Ronald Francis
.....
Dr. Ronald Francis

October 25, 1982
.....
(Date)

THESIS RELEASE PERMISSION FORM

ROCHESTER INSTITUTE OF TECHNOLOGY
COLLEGE OF GRAPHIC ARTS AND PHOTOGRAPHY

Title of Thesis MATHEMATICAL MODELING OF BLACK-AND-WHITE CHROMOGENIC
IMAGE STABILITY

I, Charles Philip Datema, hereby grant permission to the Wallace Memorial Library of R.I.T. to reproduce my thesis in whole or in part. Any reproduction will not be for commercial use or profit.



Date 13 September 1982

ACKNOWLEDGEMENTS

Completion of this thesis was only possible because of the technical support and encouragement provided by many individuals:

Mr. Milton Pearson of the R.I.T. Research Corporation who kindly consented to act as thesis advisor for this project.

Mr. Irving Pobboravsky, R.I.T. Research Corporation, whose regression analysis programs, many of which he tailored for this thesis, were invaluable.

Mr. Herbert Philips, R.I.T. Technical and Education Center, who kindly provided his organization's spectrophotometer to assist in this effort.

Professor John F. Carson for his encouragement and spectral programs which he willingly provided.

My wife Susan, as well as Jay and Jonathan, without whose encouragement and sacrifice this study would not have been completed.

The support of the Air Force Institute of Technology is also acknowledged.

TABLE OF CONTENTS

I. Introduction	1
1. General	1
2. Measurement of Image Stability	2
3. Fading Mechanisms	3
4. Research Objectives	4
II. Experimental Procedure	6
1. Time-Temperature-Humidity Model	6
2. Additivity of Light and Dark Fading	8
3. Relative Stability of Agfapan Vario-XL	10
a. Dark Fading Conditions	10
b. Light Fading Conditions	13
III. Discussion of Results	15
1. General	15
2. Time-Temperature-Humidity Series	18
a. General	18
b. Analysis of Variance	18
c. Regression Analysis	21
(1) Univariate Models	22
(2) Bivariate Models	25
(3) Trivariate Model	26
d. Arrhenius Relationship	27
3. Additivity of Light and Dark Fading	39
a. Conditions for Additivity	39
b. Experimental Results	41
4. Relative Stability of Agfapan Vario-XL	44
a. Dark Stability	44
b. Light Stability	48
c. Effect of Image Fade	49
IV. Conclusions	52
V. List of References	55
VI. Appendicies	59
1. Appendix A. Solutions for Maintaining Constant Relative Humidity	60

2.	Appendix B. Spectral Data and TI 58C/59 Program for Calculating Printing Density	61
3.	Appendix C. Calibration of Source for Light Stability Tests	63
4.	Appendix D. Intervalometer Schematic	65
5.	Appendix E. Average Transmittance Values Measured at 680nm for Dark Fading Conditions	66
6.	Appendix F. Analysis of Variance (ANOVA) Calculations	67
7.	Appendix G. Univariate Equations for Dark Fading	69
8.	Appendix H. Bivariate Equations for Dark Fading	72
9.	Appendix I. Spectral Power Distribution of Enlarger Source (Combination of Lamp and Condenser)	74
10.	Appendix J. Product of Polycontrast Filter Response and Kodak Polycontrast Rapid II RC Paper Sensitivity	75
VII.	Vita	76

LIST OF TABLES

<u>Table Number</u>		<u>Page Number</u>
1.	Outline of Experimental Flow.....	5
2.	Significance of Primary Variables and Interaction Terms.....	19
3.	Components of Variance Analysis.....	20
4.	Kinetics Models.....	29
5.	Second-Order Rate Constants and Correlation Coefficients.....	32
6.	Comparison of Two Arrhenius Methods for Predicting Dark Fade of Cyan Dye.....	38
7.	Linear Correlation Coefficients for Cyan Dye Light and Dark Fading.....	41
8.	Total Change in Transmittance for Three Test Conditions at 450nm, 540nm, and 680nm.....	43
9.	Arrhenius Predictions for 10% Loss in Printing Density at Various Relative Humidity Storage Conditions.....	47
10.	Printing Contrast for Unfaded and Dark Faded Negative.....	50

LIST OF FIGURES

<u>Figure Number</u>		<u>Page Number</u>
1.	Spectral Density Curve for a Typical Three-Component Chromogenic System	6
2.	Cascaded Values of Power Source, Optics Transmittance, and Paper Sensitivity	12
3.	Spectrophotometric Transmittance Curve Depicting Dark Fading at Various Time Intervals at Low Humidity (20% RH)	16
4.	Spectrophotometric Transmittance Curve Depicting Dark Fading at Various Time Intervals at High Humidity (80% RH)	16
5.	Spectrophotometric Transmittance Curve Depicting Light Fading	17
6.	Univariate Relationships between Delta Trans- mittance and Temperature, Humidity, or Fade Time	23
7.	Relationship between Change in Density (ΔD) and Fade Time	24
8.	Relationship between Fade Time and Transmittance, T, Density (D), Log D, $1/D$, and $1/D^2$	31
9.	First and Second-Order Correlation Coefficients as a Function of Relative Humidity	33
10.	Arrhenius Plot (First-Order) for 20% RH Dark Keeping of Cyan Dye	35
11.	Arrhenius Plot (Second-Order) for 80% RH Dark Keeping of Cyan Dye	35
12.	Dark Fading of Cyan Dye at Different Temperatures from an Initial Density of 1.0	36

<u>Figure Number</u>		<u>Page Number</u>
13.	Predicted Dark Fading of Cyan Dye at Different Temperatures from an Initial Density of 1.0	37
14.	Requirement for linear and Non-Interactive Rate Constants for Light and Dark Fading	39
15.	Results of Non-Linear Rate Constants for Light and Dark Fading	40
16.	Graphs of Actual Cyan Dye Light and Dark Fade Rates	41
17.	Change in Film Transmittance after Light and Dark Fading	42
18.	Printing Density with Respect to Fade Time at Various Temperatures	45
19.	Predicting Dark Fading (Printing Density) at Different Temperatures for Film Stored at 20, 45, 60, and 80 Percent Relative Humidity	46
20.	Change in Printing Density after Exposure to Enlarger Light for 45 Hours	48

INTRODUCTION

1. General

The design of color photographic systems has traditionally emphasized such factors as emulsion speed, resolution, tone reproduction, ease of processing, and cost.¹ Within the past 15 years image stability has emerged as a prominent design criteria. This increased attention to image stability has stemmed from studies that have challenged the stability of the dyes used in most color processes.²

Black-and-white films, on the other hand, based on the reduction of silver halide emulsions, are extremely stable, relative to color emulsions, and with proper processing and storage are often considered archival permanent.^{3,4} The fundamental technology of silver halide black-and-white films, aside from special purpose applications and diffusion transfer processes, has changed very little during this century. Recently, however, Agfa-Gevaert and Ilford have introduced black-and-white films based on dye systems corresponding to those used in color photographic films. Similar to color films, these new emulsions contain color couplers which react with oxidized developer to yield various dyes. By combining color couplers a nearly neutral negative image is formed. According to manufacturers' claims, the

new "chromogenic black-and-white" films offer an extremely high speed-to-grain ratio, wider exposure latitude, with the added feature that virtually all silver in the emulsion can be recovered from the processing chemistry.^{5,6,7} Yet, depending upon the particular application, these advantages could be off-set by the relative instability of the dye image.

2. Measurement of Image Stability

An attempt to standardize measurement of dye image stability was undertaken by Hubbell, McKinney, and West of Eastman Kodak Company in 1967.⁸ Their test procedures were later incorporated in the American National Standards Institute PH 1.42-1 1969.⁹ The standard established various accelerated test procedures, which are intended to closely simulate the actual conditions of product use. The standard also specifies that sensitometric exposures are prepared using normal processing instructions. Integral density measurements are made before and after the dye stability test using appropriate narrow-band red, green, and blue filters (e.g., Kodak Status A filters) whose transmittance curves peak close to the maximum absorption regions of the three dyes in the color film.¹⁰ Hubbell et al recommended spectrophotometry be employed when a more thorough investigation of the hue shifts, stain, or print-out is required.¹¹

3. Fading Mechanisms

Dye image fading is divided into two categories:¹² Light fading refers to the photochemical processes resulting from exposure to light. Both the intensity and the wavelength distribution of the radiation are important. Dark fading refers to the chemical changes that occur without irradiation, which result in a density loss (or transmittance gain) in the photographic material. Heat and humidity are the two primary factors which influence the chemical reactions and image degradation. Atmospheric constituents (e.g., sulfur oxides, nitrogen oxides, and ozone) are also factors in dark fading but in general are not as significant as temperature and humidity.¹³ Earlier studies have confirmed that dark fading reactions are primarily of two types: hydrolytic and oxidative-reductive.¹⁴ As would be expected, both reaction types are sensitive to temperature and humidity. Because light fading and dark fading result from photochemical and chemical reactions, respectively, it is often assumed that these two reactions are independent, and the total observed image fade is merely the mathematical sum of the two fade mechanisms.¹⁵ Experimental evidence for this assertion, however, is not conspicuous in the literature.

Similarly, published literature provides very little insight to mathematical modeling which relates fading to fade time, humidity,

and temperature. The Arrhenius model, which relates fade rate to temperature by plotting reaction rates as a function of absolute temperature is widely recognized, and it is generally assumed that the fading of color dyes increases with increasing humidity.¹⁶ However, the empirical relationship between fading and humidity as well as interactions between temperature, humidity, and fade time are not reported.

4. Research Objectives

The objective of this research is to examine the image stability of Agfapan Vario-XL black-and-white chromogenic film; specifically, (1) to determine mathematical models which define dark fade with respect to fade time, temperature, and humidity, (2) to test the hypothesis that light and dark fading mechanisms are independent and thus additive, and (3) to assess the relative image stability of the film by predicting the time required for a perceptable change in its printing density under normal dark and light fading conditions. The report generally discusses each of these three objectives separately so that each could be read independently or considered as part of the common study. Table 1 outlines the experimental flow.

Table 1. Outline of Experimental Flow

- I. Time-Temperature-Humidity Model: Relates the effect of fading time, temperature, and relative humidity to change in film transmittance.
 - A. Analysis of Variance (ANOVA): Statistically tests the significance and interaction of time, temperature, and humidity.
 - B. Components of Variance Analysis: Determines the relative effects of time, temperature, and humidity.
 - C. Regression Analysis: Fits the data to mathematical equation.
 1. Univariate
 2. Bivariate
 3. Trivariate
 - D. Arrhenius Relationship: Predicts the fading rate at room temperature by extrapolating accelerated rates obtained at high temperatures.
- II. Additivity of Light and Dark Fading Mechanisms: Tests the hypothesis that light and dark fading reactions are independent and additive.
- III. Relative Stability of Agfapan Vario-XL Film:
 - A. Dark Keeping: Arrhenius Method used to calculate time required to obtain a ten percent reduction in printing density from initial density of 1.1 at different relative humidity levels.
 - B. Light Keeping:
 1. Continuous Exposure: Determine the magnitude of fade using continuous exposure.
 2. Intermittent Exposure: Determines the magnitude of fade using an intermittent exposure.

EXPERIMENTAL PROCEDURE

1. Time - Temperature - Humidity Model

For this portion of the study, fading of only the cyan dye was modeled. This is due to the fact that only integral densities can be measured for the dye absorption spectrum where yellow and magenta dyes are absorbed. Figure 1, which is a typical integral spectral density curve for chromogenic systems,¹⁷ illustrates this point.

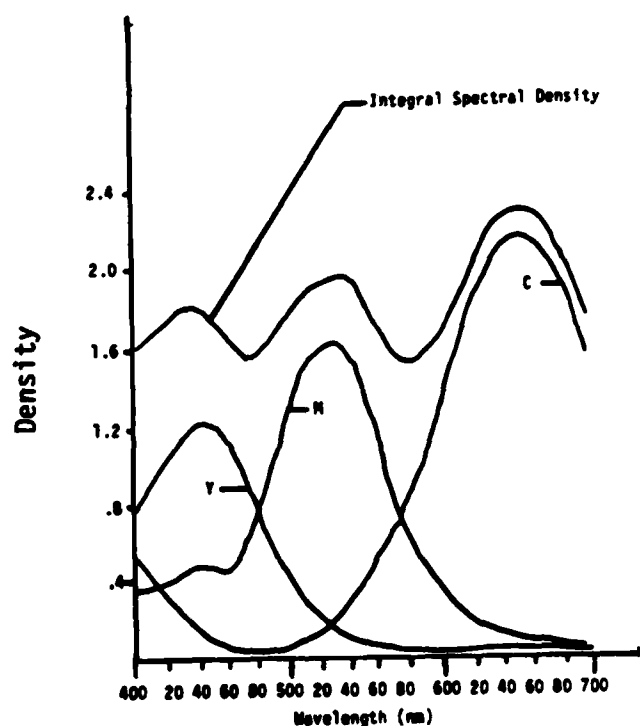


Figure 1. Spectral Density Curve for a Typical Three-Component Chromogenic System

Between 400 and 680 nm measured densities are a contribution of primary absorption from either yellow, magenta, or cyan dye, as well as secondary absorption from the other two dyes. Beyond 680 nm measured densities result essentially from primary absorption of the cyan dye; i.e., integral and analytical densities are nearly equal. Unlike conventional color systems, analytical densities between 380 and 670 nm for black-and-white chromogenic systems cannot be easily derived from integral densities because all silver halide grains are sensitized throughout the entire visible spectrum. Thus, only the cyan dye can be modeled without physically removing the other two dyes.

A Kodak 101 Process Control Sensitometer was used to expose the film (Lot Nos. 103 and 105) and the film was processed using Kodak C-41 chemistry as recommended by the film manufacturer.¹⁸ Processing times and temperatures were as outlined in Kodak Flexicolor processing instructions, KP Ø 66761g 9-80. The exposure aim point was such that the minimum transmittance of the cyan dye measured relative to unexposed film base with a Beckman DK-2A spectrophotometer was between 0.09 and 0.12. This aimpoint was somewhat arbitrary but corresponds to initial densities used by Bard, Larson, and Hubbell in their studies.¹⁹ The transmittance of the exposed film emulsion was approximated by measuring spectrophotometric transmittance relative to unexposed, but processed, film. Changes in D_{\min} due to fading and coloration of the film

base were also eliminated by taking all measurements relative to the film base.

After exposure, processing, and spectrophotometric measurement the film was faded by incubating in desiccators, which were placed in thermostatically controlled convection ovens for various time periods. The relative humidity within the desiccators was regulated by saturated salt solutions to yield a specific relative humidity within a given temperature range. Appendix A lists the inorganic salts and describes the temperature-humidity relationship used in this experiment. Four relative humidity levels (approximately 20, 45, 60, and 80 percent), and four temperature levels (68, 77, 85, and 93°C) were used, and transmittance measurements were recorded at various intervals. Transmittance measurements were taken, at a minimum, following two, four, and seven day's incubation and thereafter every seven days until at least a twenty percent change in transmittance (ΔT) was observed. Generally a much greater ΔT was obtained before terminating a particular test. A sample size of at least two (duplicates) was used for each test.

2. Additivity of Light and Dark Fading

To test the hypothesis that light and dark fading are independent, and thus additive, fourteen film strips were sensitometrically exposed

and processed to yield a minimum integral yellow dye transmittance between 0.27 and 0.30, measured relative to unexposed film. Four test strips were incubated under accelerated dark fading conditions for 21 days at 68°C and 20 percent relative humidity. Spectrophotometric measurements were made prior and subsequent to treatment. After measurement, the dark faded test strips plus the ten remaining strips^a were irradiated by a General Electric H400A33-1/T-16 medium pressure Mercury vapor lamp at a distance of 25 cm. Measured envelope irradiance at the film surface was 6400 ft-candles. Spectral dye transmittance curves were again measured, and foil covered test strips were used to approximate any dark fading which would occur during exposure due to elevated temperatures caused by the mercury vapor lamps. The above procedure created three test conditions:

- (1) Samples were incubated at constant temperature and humidity, while others were irradiated and the separate effects were added. ($F_{\text{dark}} + F_{\text{light}}$)
- (2) Samples were irradiated then incubated at constant temperature and humidity. ($F_{\text{light}} \rightarrow F_{\text{dark}}$)

a. Determination of sample size was based upon a statistical estimate using earlier measurement of experimental variance.²⁰

- (3) Samples were incubated at constant temperature and humidity then irradiated ($F_{\text{dark}} \rightarrow F_{\text{light}}$).

If light and dark fade mechanisms are indeed additive or independent as suggested by the literature,²¹ each of the three conditions should yield the same total fade as measured by total change in transmittance.

3. Relative Stability of Agfapan Vario-XL

Of practical significance to the professional, as well as the amateur photographer is the relative dark keeping properties of black-and-white chromogenic films under normal keeping conditions. A corollary question has arisen as to whether ordinary levels of irradiation from a photographic enlarger produces a significant change in film transmittance.²²

a. Dark Fading Conditions

To forecast the time required to yield a significant change in transmittance under dark keeping conditions, data from the time-temperature-humidity experiment was used. To more directly demonstrate the effect of a change in transmittance, film transmittance data were transformed to printing density using the following relationship:

$$D_p = -\log_{10} \frac{\int E_\lambda S_\lambda O_\lambda T_\lambda d\lambda}{\int E_\lambda S_\lambda O_\lambda d\lambda} \quad \text{where}$$

E_λ = Relative spectral radiant power of enlarger source at λ

T_λ = Transmittance of negative at λ

O_λ = Transmittance of enlarger optical system exclusive of the negative at λ

S_λ = Spectral sensitivity of photographic paper at λ

An Omega D-6 enlarger, equipped with a Kodak Ektar OR 218 50mm lens and a GE PH212 150w lamp, was used during the experiment to fade the film and is considered to be representative of those used to print 35mm negatives. For printing density calculations the spectral radiant power of a 3000⁰K enlarger source and a standard paper sensitivity were used.²³ The transmittance of the enlarger optics system was determined by dividing the spectral power distribution of the enlarger measured at the enlarger baseboard by the spectral power distribution of the enlarger lamp. These measurements were made at 10nm increments using an EG&G radiometer/micrometer/filter wheel system. Appendix B lists the relative values for E_λ , S_λ , and O_λ , and Figure 2 graphically illustrates the cascaded values of E_λ , S_λ , and O_λ , which indicate the relative sensitivity of the enlarger-paper system, at various wavelengths, to changes in film transmittance. A program for determining

D_p for this system using a Texas Instrument 58C/59 is also included in Appendix B.

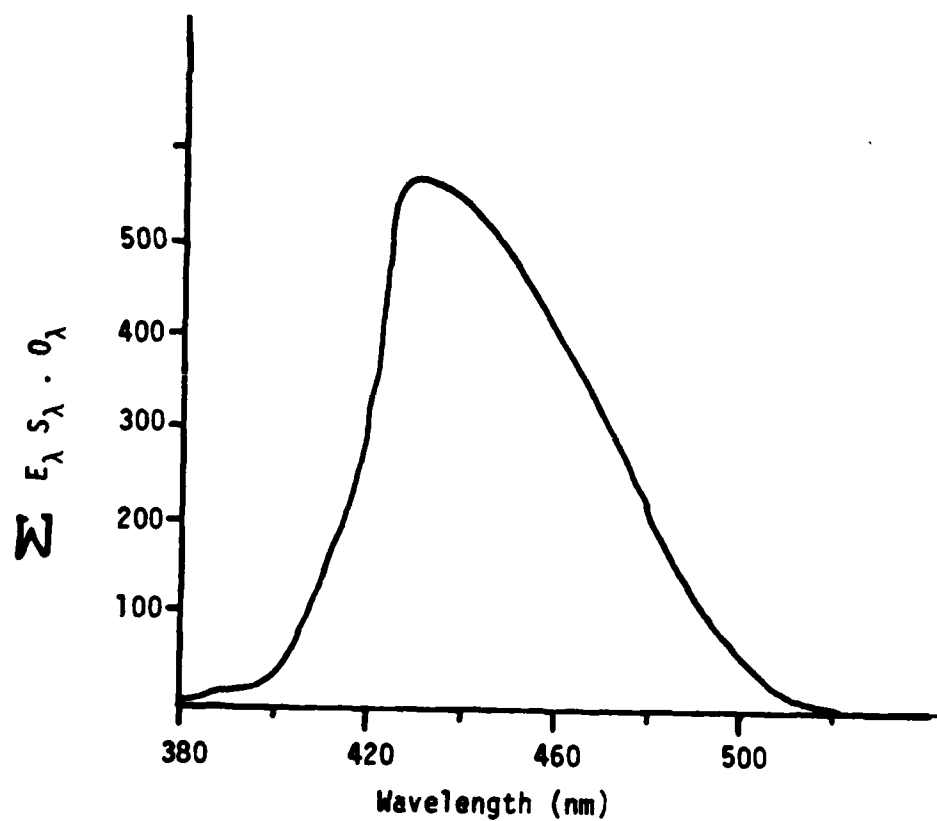


Figure 2. Cascaded Values of Power Source, Optics Transmittance, and Paper Sensitivity

After transforming film spectral transmittance values to printing densities, predictions of the time required for negatives to lose ten percent of original printing density at room temperature were obtained by using the Arrhenius relationship and extrapolating the fade rates at accelerated temperatures to normal rates at room temperature.

b. Light Fading Conditions

To investigate the light stability of the film when subjected to enlarger irradiance during printing, the exposed Agfapan Vario-XL film was placed in the Omega D-6 negative carrier, emulsion toward the enlarger base, and irradiated by the enlarger for 45 hours. This exposure time is equivalent to 9530 17-second exposures of the negative--far more printing exposures than the average negative would be subjected to. Irradiance at the film plane was 472 foot-candles with a distribution temperature of 3100°K . After 45 hours exposure the irradiance from the tungsten source decreased to 445 foot-candles. Procedures for calibrating and measuring light sources are contained in Appendix C.

Four test strips were irradiated. To approximate the portion of the total fade which was attributed to only dark fade (chemical reaction) due to heat build up, two control strips, exposed the same as

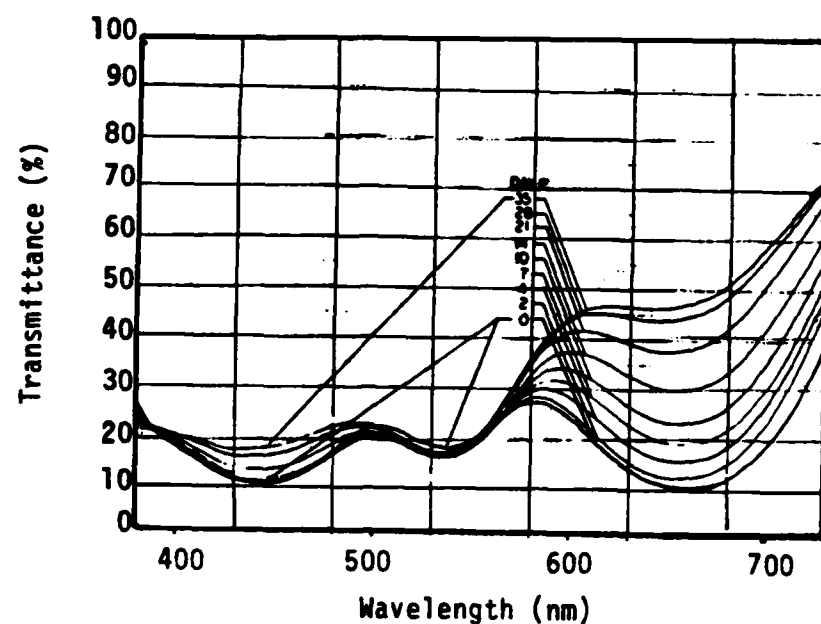
the test strips, were wrapped in aluminum foil and placed in the enlarger negative carrier with the test strips. The average change in transmittance of these control strips was subtracted from the total change in transmittance of the test strips.

Recognizing that a significant intermittency effect would bias the experiment as a measure of the film's light stability under actual conditions of use, an intervalometer was designed and fabricated. The intervalometer had a on-cycle of 17 seconds followed by a 56-second off-cycle. The cycle was automatically repeated for a total exposure of 45 hours. The intervalometer schematic is listed in Appendix D.

DISCUSSION OF RESULTS

1. General

After sensitometric exposure and processing, the spectrophotometric values for each exposure were measured prior and subsequent to treatment. For dark fading tests in which film was incubated at specific temperatures and relative humidities, spectrophotometric distributions were measured at various time intervals. Figure 3 illustrates a representative case in which transmittance is measured with respect to base material. At low relative humidity (20%), the greatest change in transmittance is in the red spectral region (cyan dye), and the least change is in the blue spectral region (yellow dye). A slight decrease in transmittance (increase in density) is noted in the green spectral region (magenta dye). It must be remembered that all spectrophotometric distributions measured are integral distributions so that the decrease in green transmittance, for example, could be attributed to an actual increase in magenta dye or more likely the case, due to new reaction products from the yellow dye. At higher humidity levels (Figure 4) the same trend is noted except the relative instability of the yellow dye is much greater. From a practical standpoint, the fading illustrated in Figure 4 at high humidity is of much greater significance because most black and white papers are



predominately blue or blue-green sensitive and are insensitive to changes in film transmittance beyond 500nm.²⁴

The effect of light fading is illustrated in Figure 5. In this case the film was irradiated with a GE Photo ECT 500w photoflood lamp (Distribution temperature = 3200°K) for 20 days. The film was placed 18 inches from the lamp to yield 1700 foot-candles.

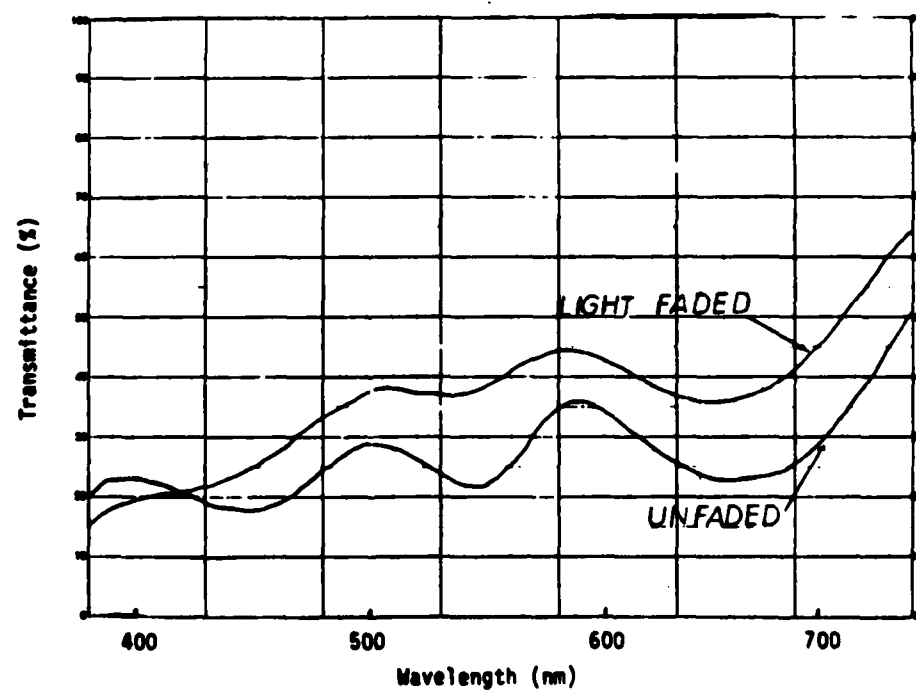


Figure 5. Spectrophotometric Transmittance Curve Depicting Light Fading

2. Time-Temperature-Humidity Series

a. General

The results of incubating the film at four levels of temperature and four levels of relative humidity were measured spectrophotometrically at various time intervals. As previously noted, mathematical modeling of the time-temperature-humidity variables was limited to the cyan dye. Although the maximum cyan dye absorption is at 660nm, measurements were recorded at 680nm to minimize secondary absorptions. Appendix E contains the average transmittance values \bar{I} , which were measured at 680nm under the various dark fade conditions at various time intervals. Each data point represents the average of at least two replicates.

b. Analysis of Variance

The replicated \bar{I} measurements for the 0, 7, 14, and 21 day intervals were analyzed using analysis of variance (ANOVA) techniques to confirm that the independent variables (fade time, temperature, and relative humidity) were statistically significant in effecting film fade. The ANOVA also determined whether significant interaction occurred between the independent variables. The C-notation algorithm

and calculation technique as specified by Rickmers and Todd²⁵ were used. The intermediate values are contained in Appendix F.

Table 2 lists the threshold value required for statistical significance for each primary variable and interaction term.

Table 2. Significance of Primary Variables and Interaction Terms

	<u>Significance Threshold</u>	<u>F-test</u>
Temperature	4.76	32.14
Relative Humidity (RH)	4.76	6.27
Fade Time	5.14	15.43
Temp X RH Interaction	2.96	10.56
Temp X Fade Time Interaction	2.66	18.17
RH X Fade Time Interaction	2.66	3.66
Temp X RH X Fade Time Interaction	1.90	6.46

The ANOVA confirmed that each variable and all interactions are statistically significant in effecting changes in transmittance as a result of dark fading conditions. The difference between the significance threshold and the F-test value indicates a measure of statistical significance.

It is not surprising that the three primary variables proved to be significant, but it was not expected that all four interactions would be significant. The interaction indicates that the amount of fade caused by one particular variable is dependent upon the magnitude

of the other two independent variables. That is to say, the effects of fade time, temperature, and humidity are not additive. This verifies that the actual fading mechanisms associated with the cyan dye are not simple and that the reaction kinetics are changing with respect to fade time, temperature, and humidity.

A components of variance analysis²⁶ was performed to determine which test variables had the greatest effect in changing film transmittance within the parameters of this experiment. Table 3 summarizes the results:

Table 3. Components of Variance Analysis

	<u>Percent of Total Variance</u>
Temperature	67.98
Relative Humidity (RH)	5.48
Fade Time	17.75
Temp X RH Interaction	3.01
Temp X Fade Time Interaction	4.06
RH X Fade Time Interaction	0.63
Temp X RH X Fade Time Interaction	0.80
Experimental Error	0.29
TOTAL	100.00

It is readily apparent that fade time and temperature are the dominant factors within the experimental range tested, and their interaction product is the most significant interaction. Most of the other

interactions, although statistically significant, do not contribute appreciably to the total variance.

c. Regression Analysis

The fading of Variopan-XL negative material can be mathematically modeled to describe the change in negative transmittance (ΔT) as a function of fade time (t), temperature (T), and relative humidity (H). The relationship between ΔT and the independent variables may be expressed as univariate models:

$$\Delta T = f(t) \quad \text{where } T \text{ and } H \text{ are constant}$$

$$\Delta T = f(T) \quad \text{where } t \text{ and } H \text{ are constant}$$

$$\Delta T = f(H) \quad \text{where } t \text{ and } T \text{ are constant}$$

as bivariate models:

$$\Delta T = f(t, T) \quad \text{where } H \text{ is constant}$$

$$\Delta T = f(t, H) \quad \text{where } T \text{ is constant}$$

$$\Delta T = f(T, H) \quad \text{where } t \text{ is constant}$$

or as a single trivariate model:

$$\Delta T = f(t, T, H)$$

As previously noted, there are other factors which influence fading, such as atmospheric constituents, but these other factors were essentially constant during the experiment and are not included in the model.

(1) Univariate Models

The \underline{I} data points from Appendix E can be converted to $\Delta \underline{I}$ by subtracting from each value the initial, or Day 0, \underline{I} value. These $\Delta \underline{I}$ values can then be plotted to indicate the relationship between $\Delta \underline{I}$ and fade time, temperature, or relative humidity. With three levels of fade time and four levels each of temperature and humidity a total of $40 \left((4 \times 4) + (4 \times 3) + (4 \times 3) \right)$ univariate, or one-dimensional, relationships exist.

In Figure 6, 15 of these univariate equations are plotted in four families of curves. The equations were derived using a least squares regression analysis program which calculates linear, exponential, logarithmic, power, second-order polynomial and third-order polynomial regression models. In nearly every case the second-order polynomial ($y = a + bx + cx^2$) provided the best fit (highest correlation coefficient and lowest standard error). All univariate equations, including those for the graphs in Figure 6 are listed in Appendix G.

Several conclusions can be reached from the univariate relationships:

First, within the range of this experiment, the fading of the

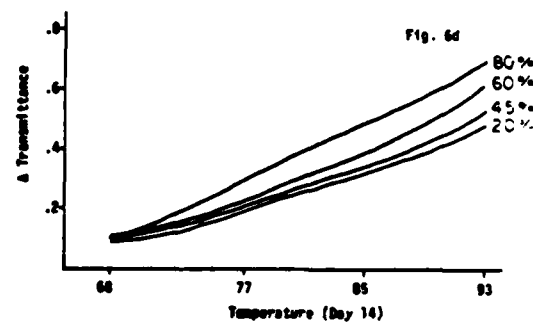
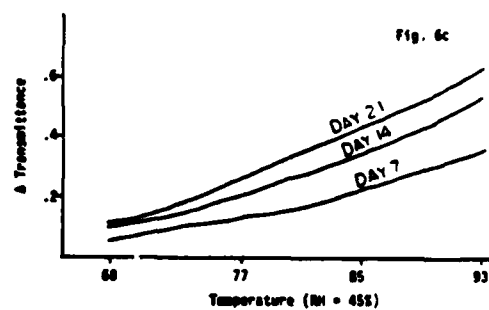
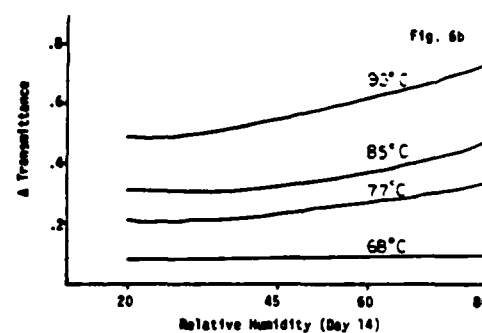
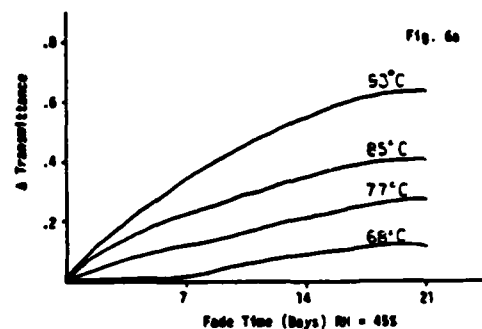


Figure 6. Univariate Relationships between Change in Transmittance (ΔT) and Fade Time, Relative Humidity, and Time.

cyan dye can be closely modeled using second-order univariate relationships. The average correlation coefficient for the 40 models is 0.976, and the average standard error is 0.0174.

Second, the rate of fade ($\Delta T/\text{time}$) is not constant. (Figure 6a). If the original transmittance data were converted to density ($D = -\log_{10} I$), and if ΔD were plotted with respect to time, the rate of fade $\Delta D/\text{time}$ is even more variant. Figure 7, for example, shows a typical relationship between ΔD and time. This point will be further developed when the Arrhenius relationship is discussed.

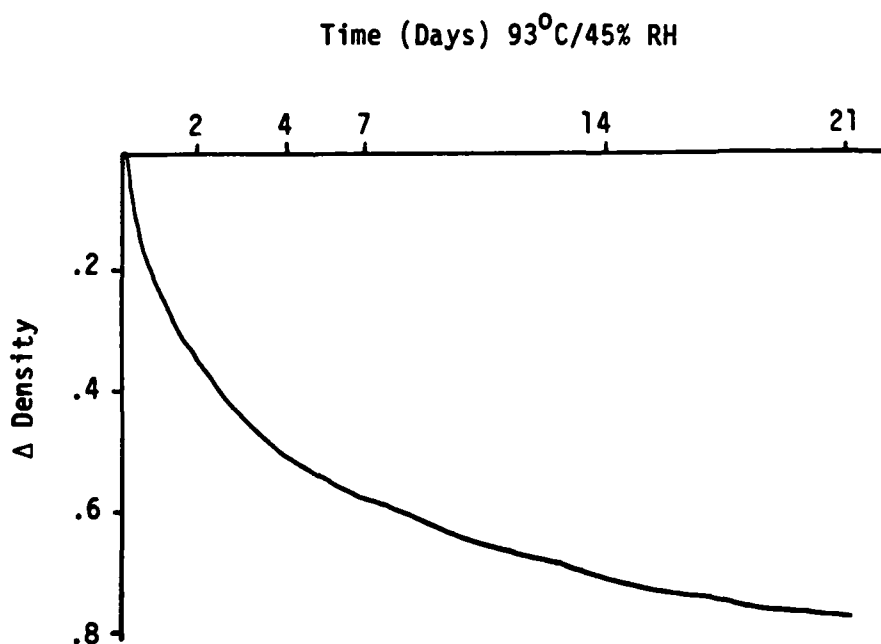


Figure 7. Relationship between Change in Density (ΔD) and Fade Time.

Third, for this particular cyan dye, the effect of humidity at low temperatures (68°C) is insignificant (Fig. 6b.). At room temperature, humidity would not be expected to be significant. The effect of humidity is much greater at higher temperatures, due to the interaction between humidity and temperature.

Finally, the interaction of independent variables, which the analysis of variance proved to be statistically significant, is substantiated in each of the graphs. Without interaction, each of the plots within families of curves would be parallel.²⁷

(2) Bivariate Model

The fading model may also be expressed as a more general bivariate equation in which ΔI is described as a function of time and temperature, time and humidity, or temperature and humidity. In each case the third independent variable is held constant. The optimal two-dimensional equation for each bivariate form was determined using a least squares program developed by I. Pobboravsky, R.I.T. Research Corporation. The program calculated the coefficients for the two independent variables as well as correlation coefficients and standard errors for the bivariate models in three forms:

$$y = a_0 + a_1x_1 + a_2x_2$$

$$y = a_0 + a_1x_1 + a_2x_2 + a_3x_1x_2$$

$$y = a_0 + a_1x_1 + a_2x_2 + a_3x_1^2 + a_4x_2^2 + a_5x_1x_2$$

where

y = the dependent variable

x_1 and x_2 = the independent variables

In each instance, the third equation (second-order with interaction term) provided the best fit yielding the largest correlation coefficient and the smallest standard error. This further suggests that the fading rates are second-order and that interaction between the factors exists. The various bivariate equations are listed in Appendix H. The average bivariate equation correlation coefficient was .974 and the average standard error was 0.0369.

(3) Trivariate Model

To develop a more general mathematical model of the cyan dye fade a second-order trivariate regression model of the following format was introduced:

$$\begin{aligned} \Delta T = & a_0 + a_1t + a_2T + a_3H + a_4t^2 + a_5T^2 + a_6H^2 + a_7tT \\ & + a_8tH + a_9TH \end{aligned}$$

It should be noted that this ten-term, trivariate model includes all factors and interactions that the ANOVA proved to be significant with the exception of the third-order interaction between time, temperature and humidity. Since this third-order interaction contributed only 0.8 percent of total variance, its omission from the model is not significant. A least squares program developed by I. Pobboravsky fit the data in Appendix E and yielded the following trivariate equation:

$$\begin{aligned}\Delta T = & 1.2764 - 0.0564t - 0.0294T - 0.0104H - 6.0660 \times 10^{-4} t^2 \\ & + 1.7312 \times 10^{-4} T^2 + 2.7241 \times 10^{-5} H^2 + 1.0090 \times 10^{-3} tT \\ & + 1.3445 \times 10^{-4} tH + 1.0004 \times 10^{-4} TH\end{aligned}$$

The model provided a correlation coefficient of 0.9592 and a standard error of 0.0438.

d. Arrhenius Relationship

The relationship between the rate of many chemical reactions, such as fading, and temperature can be represented by an empirical equation proposed by Arrhenius.²⁸

$$\frac{d(\ln k)}{dT} = \frac{E}{RT^2}$$

where k = the rate constant for the reaction

R = the universal gas constant

T = the absolute temperature

E = the activation energy for the reaction

Assuming the activation energy is independent of temperature, the equation can be integrated to

$$\ln k = \frac{-E}{RT} + C$$

where C is the integration constant. Since E and R are assumed to be independent of temperature, $\ln k \propto 1/T$. By plotting $\ln k$ versus $1/T$ a straight line should be obtained with a slope equal to $-E/R$. By extrapolating this straight line to room temperature, normal fading rates may be predicted from accelerated aging tests conducted at higher temperatures.

Key to the Arrhenius equation is application of the proper rate constant for the fading mechanism; the rate constant must indeed be constant with respect to time.

The rate constant of any chemical reaction depends on the kinetics of the reaction. In general, the rate is dependent upon the concentration of the reactants, and the differential equation expressing the rate as a function of the concentration of each of the species which affect the rate is called the rate law of the reaction. For

example, for a reaction with reactants A and B, the rate law could have one of the following forms:²⁹

$$\text{First Order in A: } \frac{-d(A)}{dt} = k(A) \text{ or } k(A)(B)$$

$$\text{Second Order in A: } \frac{-d(A)}{dt} = k(A)^2 \text{ or } k(A)^2(B)$$

$$\text{Third Order in A: } \frac{-d(A)}{dt} = k(A)^3 \text{ or } k(A)^3(B)$$

$$\text{Zero Order in A: } \frac{-d(A)}{dt} = k(A)^0 = k$$

The order of a particular chemical reaction may be determined by plotting different functions of the concentration (c) versus time.

Table 4. Kinetics Models

<u>Reaction Order</u>	<u>Straight Line Plot</u>
First-Order	log c vs. time
Second-Order	1/c vs. time
Third-Order	1/c ² vs. time
Zero-Order	c vs. time

A more detailed explanation of reaction order, as well as a derivation of the relationships above, may be obtained from any chemical kinetics or physical chemistry text.^{30, 31}

The relationship between the concentration of the reactants (dyes) that affect the fading rate constant and density is explained by the Lambert-Beer law³²

$$I = I_0 10^{-ecx}$$

where e = dye extinction coefficient
 c = concentration
 x = thickness
 I = transmitted light
 I_0 = incident light

Since transmittance, \underline{T} , equals I/I_0 , and density (D) = $-\log_{10} \underline{T}$, it follows that

$$D = \log_{10} 1/\underline{T} = ecx$$

Since e and x are constant, density is proportional to dye concentration.

Thus, the reaction order of the fading mechanism may be determined by plotting different functions of density versus time.

Figure 8 illustrates the graphical analysis of the fading data for the 68°C/45% RH treatment. The plot of the $1/D$ versus time results in the straightest line, indicating a second-order reaction.

The slope of the line represents the reaction rate constant. Assuming this second-order Kinetic Model, linear regression analysis was performed on each treatment of temperatures and humidities for the relationship of $K = \Delta 1/D / \Delta t$.

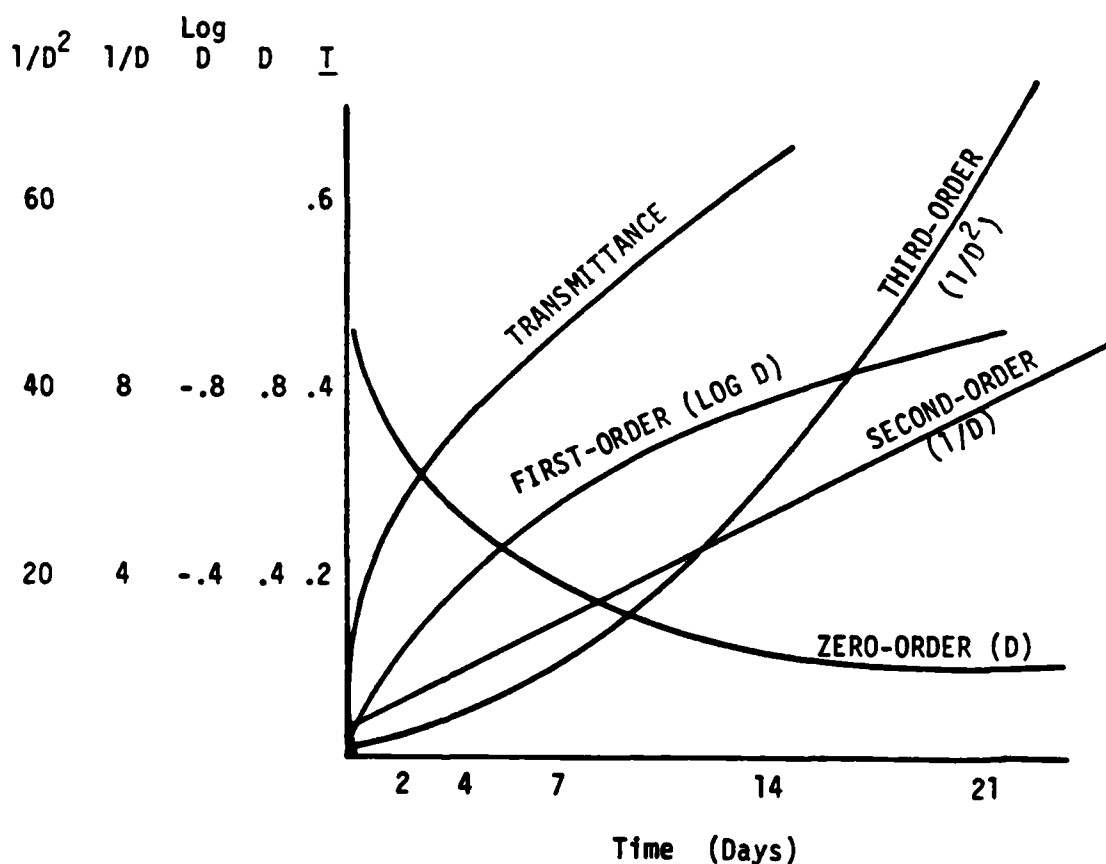


Figure 8. Relationship between Fade Time and Transmittance (T), Density (D), $\log D$, $1/D$, and $1/D^2$.

The rate constants and linear coefficients of correlation (R^2) are tabulated below.

Table 5. Second-Order Rate Constants and Correlation Coefficients

$\begin{matrix} \text{RH} \\ \text{T} \end{matrix}$	20%	45%	60%	80%
68°	.0223 ($R^2 = .997$)	.0207 ($R^2 = .991$)	.0219 ($R^2 = .980$)	.0389 ($R^2 = .989$)
77°	.0699 ($R^2 = .995$)	.0663 ($R^2 = .996$)	.1196 ($R^2 = .973$)	.1830 ($R^2 = .913$)
85°	.1095 ($R^2 = .996$)	.1175 ($R^2 = .990$)	.1520 ($R^2 = .986$)	.2902 ($R^2 = .979$)
93°	.253 ($R^2 = .999$)	.333 ($R^2 = .996$)	.5245 ($R^2 = .993$)	.8949 ($R^2 = .987$)

The second-order linear relationship models the data extremely well at lower humidity levels but not as well for 80 percent relative humidity equations. The first-order model, $k = \Delta \log D / \Delta t$, on the other hand, yielded a much better linear fit for 80 percent relative humidity data. Figure 9 plots the average correlation coefficient for the first-order as well as second-order linear models with respect to the four humidity levels.

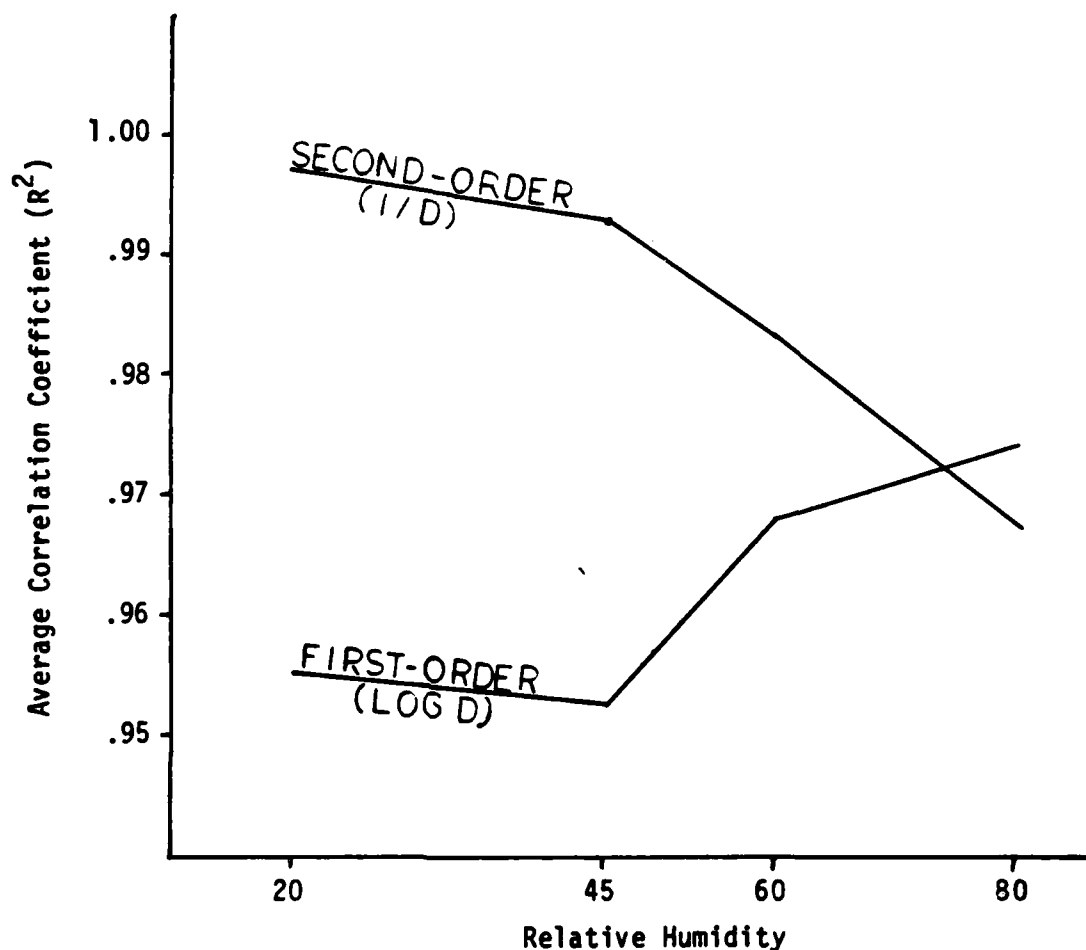


Figure 9. First and Second Order Correlation Coefficients as a Function of Relative Humidity Level.

The second-order kinetics model seems to fit the reaction kinetics except at higher humidity, at which case, a first-order model more accurately describes the reaction mechanism. A study by Y. Seoka *et al*³³ indicates that coupler solvent evaporates from photographic emulsions when relative humidity exceeds 70 percent. Previous studies by S.E. Shepard *et al*³⁴ and C.M. Martin *et al*³⁵ also suggest that the

physical properties of the gelatin layer change abruptly at about 70% RH. A correlation may exist between these findings and the apparent change in the reaction kinetics as indicated by Figure 9.

To predict the time required at room temperature (24°C) for the cyan dye to fade to a specific density, $\ln k$ is plotted against the reciprocal of the absolute temperature, and the straight line is extrapolated to room temperature. Figure 10, for example, predicts $\ln k = -9.10667$ or $k = 0.0001109$ at room temperature and 20% RH. Since the rate constant is for a second-order reaction in which $k = \frac{\Delta 1/D}{\Delta t}$, this translates to 1000 days (2 3/4-years) for a fade from $D = 1.0$ to $D = 0.9$.^a The 45% and 60% RH data predictions would not be expected to differ appreciably since earlier regression models showed that humidity is not a significant factor in the fading of the cyan dye at lower temperatures. The Arrhenius prediction, using a first-order rate constant ($\Delta \log D/\Delta t$), for a ten percent density loss from $D = 1.0$. Under 80% RH, 24°C keeping conditions is 1.5 years (Figure 11).

^a The 77° data generally did not lie on the Arrhenius $\ln k$ vs. $1/T$ straight line plots. This is attributed to an oven thermostat failure. Consequently, the 77°C data was discarded for this Arrhenius test.

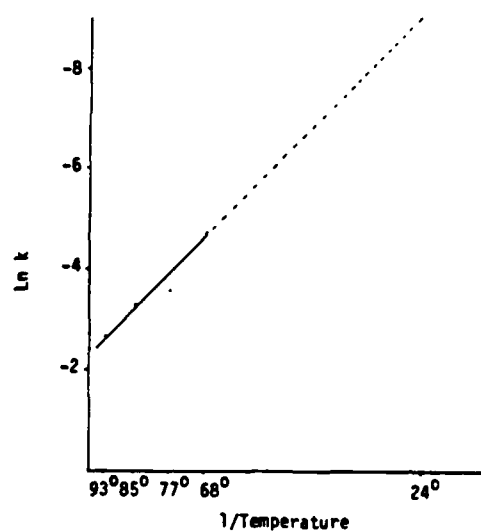


Figure 10. Arrhenius Plot (Ln k vs. 1/T) for 20% RH Dark Keeping of Cyan Dye.

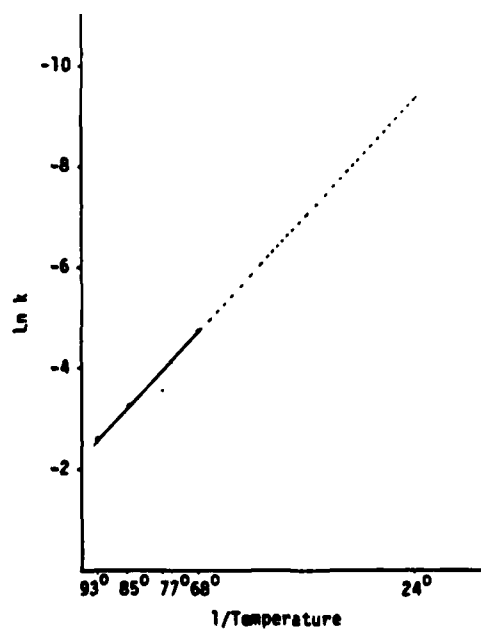


Figure 11. Arrhenius Plot (Ln k vs. 1/T for 80% RH Dark Keeping of Cyan Dye

Rather than consider the order of the fading reaction when determining the rate constant, Eastman Kodak Company authors typically assume a linear relationship between density loss and fade time.³⁶ First, density versus time curves are plotted (Figure 12). Then, from these smoothed curves the particular times required to achieve determined density losses are found for each temperature treatment. This fade time, t_T , is proportional to $1/k$, and $\ln t_T$ is plotted against $1/T$. (Figure 13)

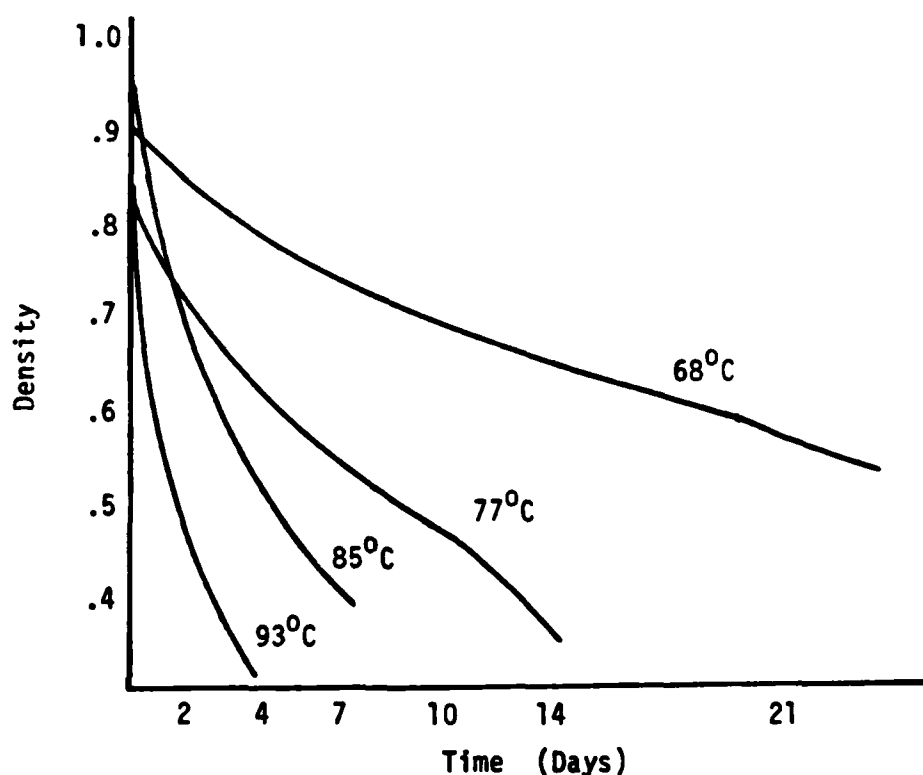


Figure 12. Dark Fading of Cyan Dye at Different Temperatures from an Initial Density of 1.0.

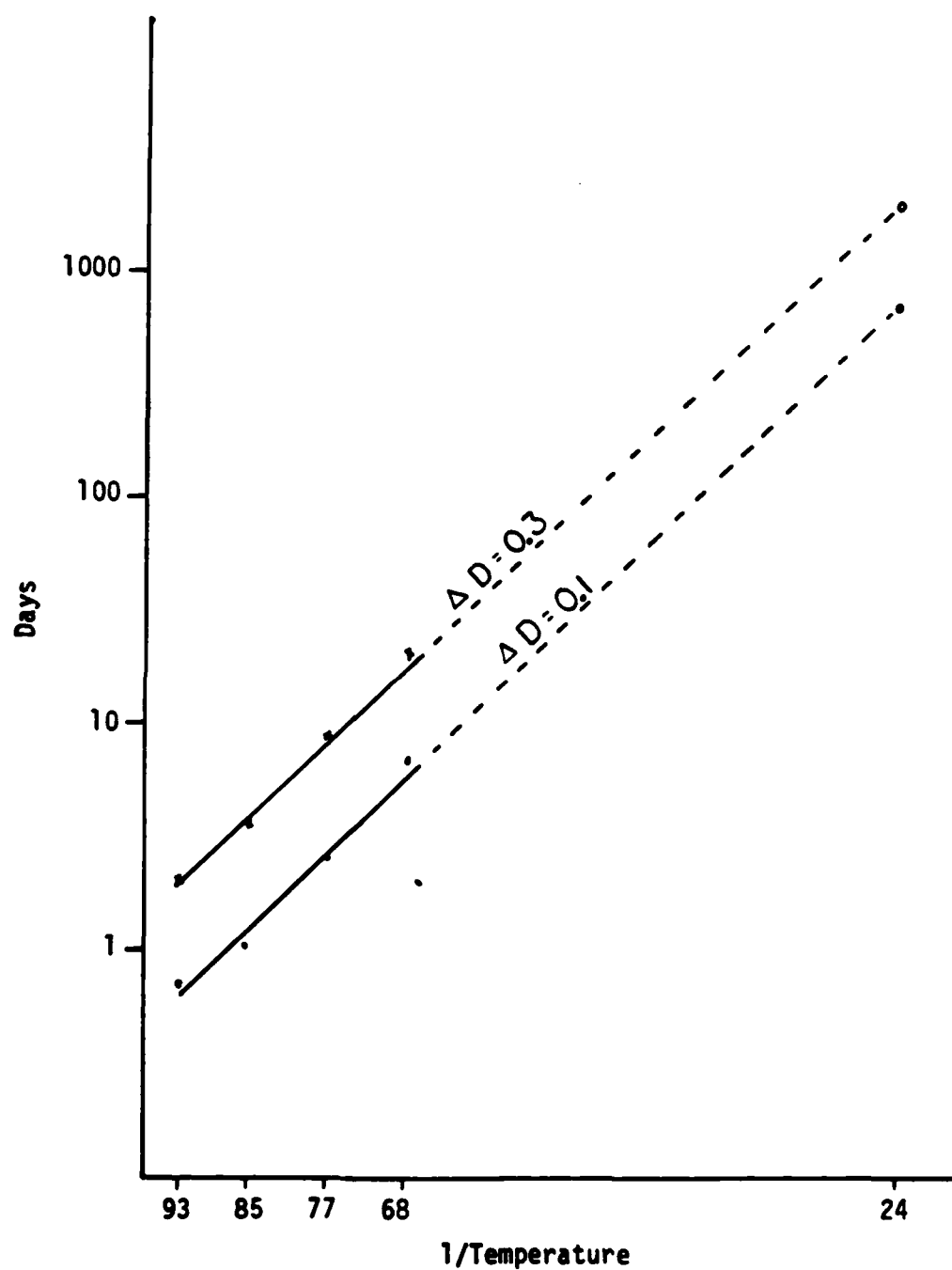


Figure 13. Predicted Dark Fading of Cyan Dye at Different Temperatures from an Initial Density of 1.0.

This particular method assumes that k is linear for a ΔD versus Δt plot, that is to say, a zero-order reaction occurs in which the rate of fade is independent of density. Figure 12 suggests that this is not the case, at least for the Agfapan Vario-XL cyan dye. The linear approximation, however, is adequate for predicting fade times for fade rates which are indeed zero-order and for small changes from initial densities. Table 6 compares the predictions from the two methods.

Table 6. Comparison of Two Arrhenius Methods for Predicting Dark Fading of Cyan Dye

	First Method (plotting $\ln k$ vs. $1/T$)	Second Method (plotting t_T vs. $1/T$)
<u>20% RH</u>		
$\Delta D = 0.1$	1000 days	700 days
$\Delta D = 0.3$	3900 days	1900 days
<u>80% RH</u>		
$\Delta D = 0.1$	543 days	500 days
$\Delta D = 0.3$	5100 days	2400 days

3. Additivity of Light and Dark Fading.

a. Conditions for Additivity

Two necessary conditions must be satisfied if the effects of light fading and dark fading are to be additive. First, there must not be any interaction between the dark fading (chemical) reaction and the light fading (photochemical) reaction. For example, products of either reaction must not function as catalysts or inhibitors for the other reaction. Second, both reaction rates must be linear. Figure 14 illustrates this second point.

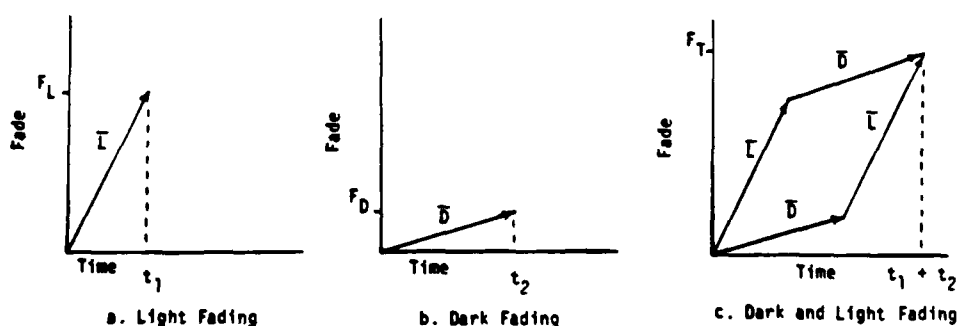


Figure 14. Requirement for Linear and Non-Interactive Rate Constants for Light and Dark Fading.

Figure 14a and 14b represent the case where individual test strips are light faded and dark faded, respectively. The total fade is obtained by adding F_L and F_D . Figure 14c represents the case where a single test strip is light faded and then dark faded ($F_L \rightarrow D$) or vice versa ($F_D \rightarrow L$). In either case, the total fade is F_T , and assuming no interaction, $F_T = F_L + F_D$. Now, if either or both reactions were not linear, as represented by Figure 15, $F_L + F_D$, $F_L \rightarrow D$, or $F_D \rightarrow L$ would not necessarily be equal.

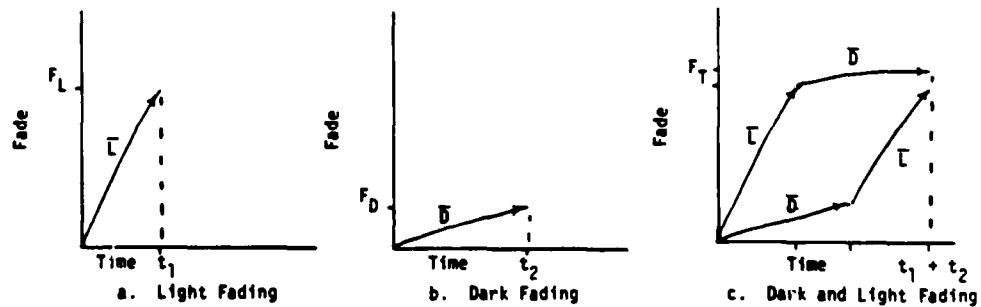


Figure 15. Result of Non-Linear Fade Rates.

b. Experimental Results

With respect to linearity, both the light fade and dark fade reactions can be considered essentially linear when plotting transmittance versus time within the range of experimental data (Figure 16).

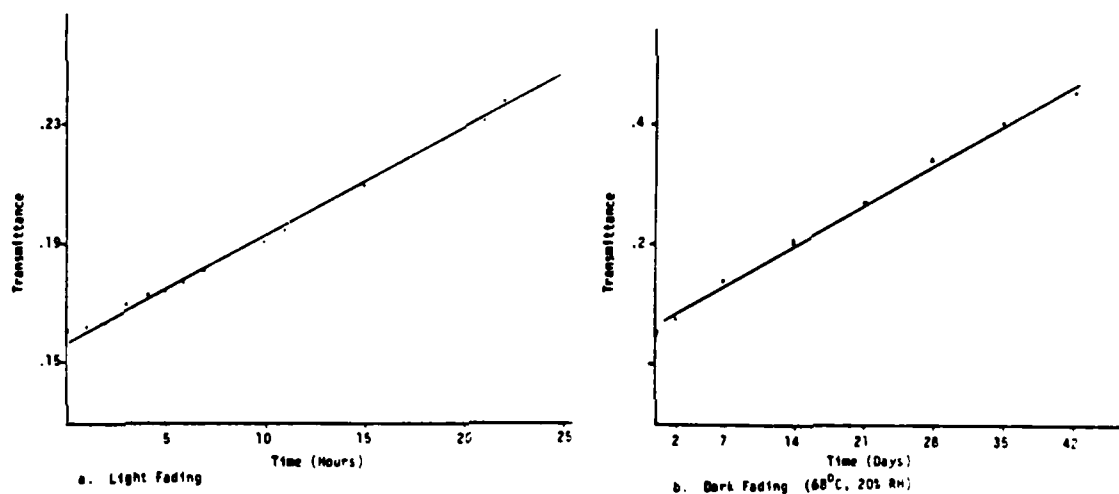


Figure 16. Graphs of Actual Cyan Dye Light and Dark Fade Rates.

The linear correlation coefficients for the light and dark reactions are as follows:

Table 7. Linear Correlation Coefficients for Cyan Dye Light and Dark Fading.

	<u>Light Fade</u>	<u>Dark Fade</u>
450nm	.980	.980
540nm	.983	.988
680nm	.990	.985

Thus, the light and dark fading rates are assumed to be sufficiently linear. It should be noted that the light and dark fade data may be transformed from I to D and $1/D$, respectively, to yield even better correlation coefficients for a linear fit. However, the final conclusions are not altered.

The changes in transmittance following treatment are shown in Figure 17, and the ΔI values at 450nm, 540nm, and 680nm are listed in Table 8.

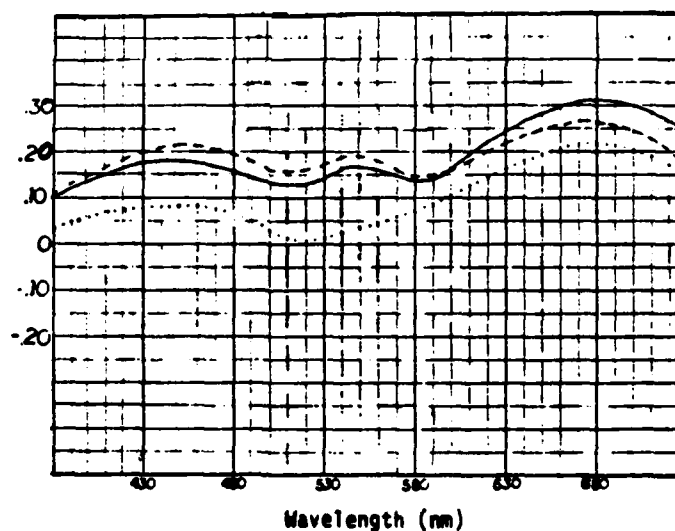


Figure 17. Change in Film Transmittance after Light and Dark Fading. Solid Line Represents $F_D + F_L$. Dotted Line Represents $F_D \rightarrow F_L$. Dashed Line Represents $F_L \rightarrow F_D$.

Table 8. Total Change in Transmittance for Three Test Conditions at 450nm, 540nm and 680nm. Values in parenthesis are individual light/dark fade components.

	<u>450nm</u>	<u>540nm</u>	<u>680nm</u>
$F_L + F_D$.1834 (.1838, -.0004)	.1636 (.1912, -.0276)	.3089 (.1519, -.1570)
$F_L \rightarrow D$.2198 (.1838, .036)	.1900 (.1912, -.0012)	.2538 (.1519, .1019)
$F_D \rightarrow L$.0824 (-.0004, .0828)	.0242 (-.0276, .0518)	.2168 (.1570, .0598)

It should be noted that the ΔT values in Figure 17 and Table 8 do not agree perfectly because the Figure 17 was derived from one representative sample, whereas the Table 8 values are the mean ΔT values from the entire experiment.

A statistical hypothesis test of the means considered the null hypothesis that $\mu_{F_L} + \mu_{F_D} = \mu_{F_L \rightarrow D} = \mu_{F_D \rightarrow L}$ using a two tailed t-test with a 0.10 critical region. The analysis failed to statistically accept the null hypothesis, which is to say, the three test conditions do not yield the same total fade. Thus, it must be assumed that there is interaction between the light and dark fade reactions.

In the case of the cyan dye (680nm), both the light and dark reactions inhibit the other reaction. In the case of the magenta (540nm)

and the yellow (450nm) dyes, a synergistic, or catalytic, effect occurs when light fading precedes dark fading. The dark reaction, however, inhibits the light reaction when the order is reversed. In each case the dominant effect is the inhibition of the dark reaction.

4. Relative Stability of Agfapan Vario-XL

a. Dark Stability

Printing densities were calculated for unfaded film and for film incubated at levels of temperature, humidity, and fade time. (Figure 18) The spectral data for calculating printing density are contained in Appendix B.

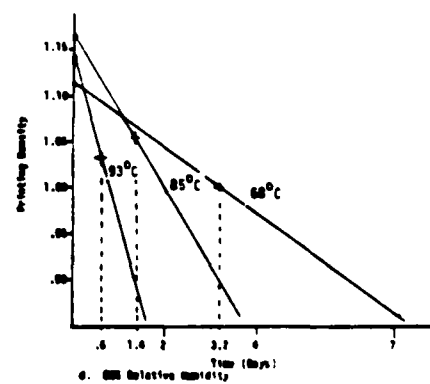
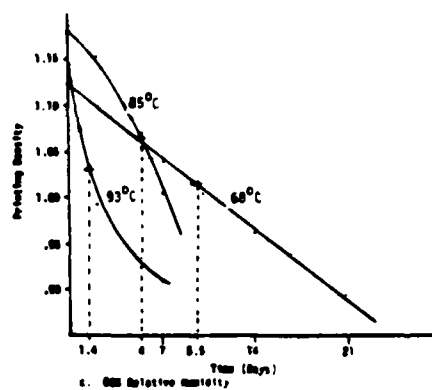
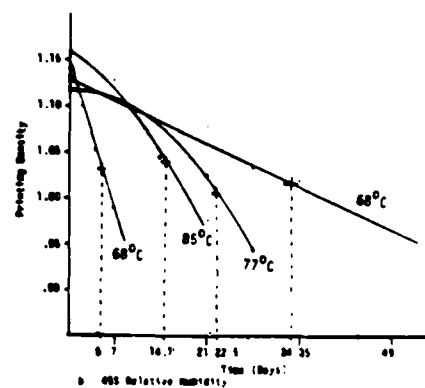
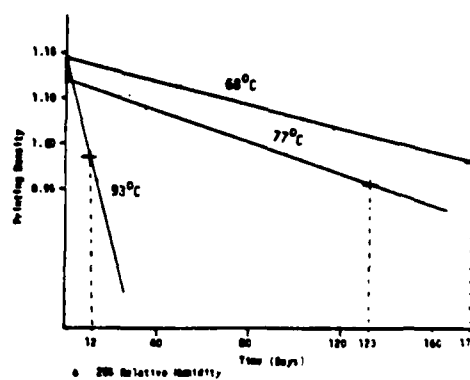


Figure 18. Printing Density with Respect to Fade Time at various Temperatures. (a) 20% RH, (b) 45% RH, (c) 60% RH, (d) 80% RH.

Since a general transformation could not be found which would create a linear fade rate for all treatment conditions, the Arrhenius methodology suggested by Kodak authors was used: The rate curves were interpolated (extrapolated for 20% tests) to determine the number of days required for a ten percent loss in density. The ten percent density loss levels are indicated in Figure 18 by the cross marks. These values were then plotted against $1/T$ on log graph paper (Figure 19) and a straight line was drawn through the points using the best visual fit.

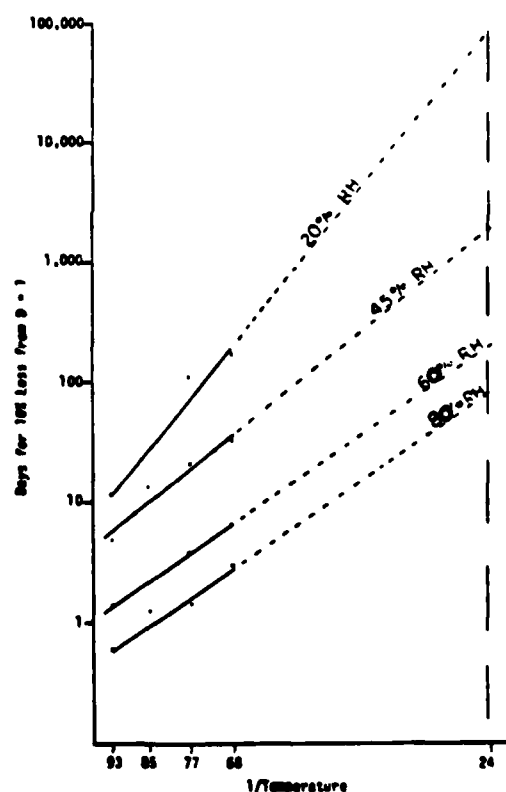


Figure 19. Predicted Dark Fading (Loss of Printing Density) at Different Temperatures for Agfapan Vario-XL stored at 20, 45, 60, and 80 Percent Relative Humidity.

Table 9 summarizes the Arrhenius predictions from Figure 19.

Table 9. Arrhenius Predictions for ten percent loss in printing density at various humidity storage conditions.

<u>Relative Humidity</u>	<u>Time for 10% loss in Printing Density</u>
20%	23 years
45%	5 years
60%	200 days
80%	80 days

Compared to Arrhenius predictions for the cyan dye, the Arrhenius projections for changes in printing density are extremely sensitive to humidity. This is because the yellow dye itself is humidity sensitive. (See Figure 4)

b. Light Stability

The change in density of the Agfapan Vario-XL after an exposure time of 45 hours is shown in Figure 20. The original printing density before fade was 0.66. The spectral power distribution of the irradiating source is shown in Appendix I.

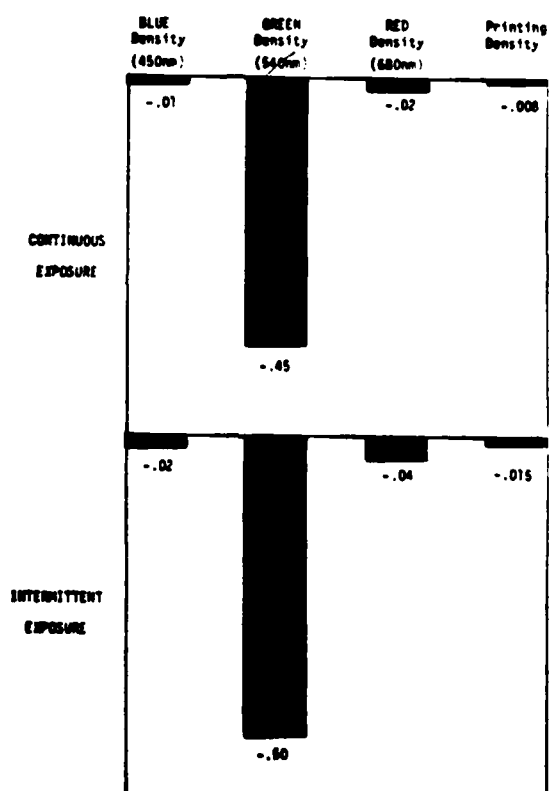


Figure 20. Change in Agfapan Vario-XL Density after 45 hour Enlarger Exposure.

From a practical standpoint, the Vario-XL is extremely light stable since at most only a 0.015 printing density loss is observed after being subjected to normal enlarger radiation for 45 hours. As previously noted, 45 hours of exposure is equivalent to more than 9000 individual 17-second exposures. An intermittency effect was observed: each dye faded more during the intermittent exposure. The effect could be more significant if the period between exposures were increased.

c. Effect of Image Fade

To a certain extent, the effect of fading of a black-and-white intermediate material is not significant for relatively large amounts of fade since color balance is not a concern and a general decrease in negative density can be compensated by reducing enlarger exposure time or lens aperture. The effect of fade, however, significantly affects printing contrast when the fading mechanism is not zero-order, since the rate constant for a zero-order reaction is independent of reactant concentration, or in this case, dye density. A non zero-order reaction mechanism would result in greater fade in high density images than in low density regions of the negative, resulting in a contrast reduction. Since this study did not address rate constants for the yellow and magenta dyes, the extent of change in printing contrast due to non-linear fading cannot be assessed.

Fading can also affect printing contrast when the dye absorption curves shift during fade, particularly when printing with multicontrast papers, which are sensitive to longer wavelength radiation. To verify this point, two Agfapan Vario-XL negatives were sensitometrically exposed with a step tablet image. One negative was dark-faded for seven days at 93°C/60% RH. The shift in absorption at 93°C/80% RH is seen in Figure 4. Both negatives were then used to print the step tablet image on Kodak Polycontrast paper using Kodak Polycontrast Filters. The resulting printing contrasts for the printed images are tabulated in Table 10.

Table 10. Printing Contrast (γ) from unfaded and faded negatives.

<u>Polycontrast Filter</u>	<u>Unfaded Negative</u>	<u>Faded Negative</u>
1	1.83	1.97
2	2.80	2.89
3	3.00	2.73
4	3.28	2.68

An interesting effect is observed when both negatives are printed with Polycontrast filter 1 which extends the paper-filter response to the magenta dye absorption region. (Appendix J shows the product of the

PC filter response-PC paper sensitivity.) In this case the build-up of the magenta dye density over-compensates for the loss of yellow dye density which results in a print with increased contrast. In the other cases, in which the filter-paper response is not extended to green radiation, the contrast from the faded negative is less, as would be expected.

CONCLUSIONS

The dark fading of the Agfapan Vario-XL cyan dye, which is assumed to be representative of most chromogenic dyes, can be accurately modeled using multiple nonlinear regression analysis. The versatility of the model increases as more variables, such as temperature, humidity, and fade time, are brought into the model, but the accuracy of the model decreases as the number of variables increases. The choice of whether to employ univariate, bivariate, or trivariate model would depend on the application - - which, if any, variables are held constant - - as well as the accuracy required. As a general rule, however, the simplest second-order equation which contains all the parameters tested would be recommended. Unlike the Arrhenius relationship, the dark fading models are only valid within the range of experimental data and cannot be extrapolated.

It was also shown that image stability modeling is complicated by simple and multiple interaction between chemical and photochemical reactions (light and dark fading are not additive), and between temperature, humidity, and fade time. Thus, precise simulation of the total fading process cannot be accomplished by isolating individual factors or without recognizing that the effect of one factor is dependent upon the level of the other factors.

The experimental data for the cyan dye generally fit the straight line Arrhenius model within the experimental temperature range. The fit was improved by transforming the data, assuming a second-order reaction for relative humidity levels below 80 percent. The 80 percent data was more linear, assuming a first-order reaction, which correlates with earlier studies suggesting the fade mechanism is rate-limited by evaporation of coupler solvent at humidities above 70 percent. As reported in the general literature, the accuracy of the Arrhenius predictions is limited when attempting to extrapolate over a large temperature range. One consequence of a long extrapolation is that two experimenters with similar rate measurements may predict dissimilar rates at room temperatures. Another consequence is that small errors caused by mechanism changes with temperature (such as coupler solvent evaporation) will bias the slope of the Arrhenius plot even though the individual rate constants are not greatly affected.

Significant interaction exists between the light and dark reactions which precludes the total fading from being additive. The dark reaction, in particular, inhibits the light reaction. Investigation of interaction between light and dark fading during simultaneous light and accelerated dark fading would be an area for further investigation.

It was also found that the film was extremely light stable when irradiated by a conventional enlarger light source. The material did exhibit an intermittency effect in which the image stability was decreased during intermittent exposures; however, the total density loss was still minimal (Figure 20).

The dark stability of the black-and-white chromogenic film compares generally with the stability of Kodacolor II color film (C-41). The time to reach a density loss of 0.10 from 1.0 original density for Kodacolor II film is reported to be six years or less.³⁷ This compares to five years for the predicted time to lose ten percent printing density for the Agfapan Vario-XL.

To compare with a black-and-white silver halide system, which more closely relates to the features of the black-and-white chromogenic film, reveals a much wider disparity in image stability. Although Eastman Kodak Company does not publish image stability data sheets for black-and-white products, it is reported that Kodak film type Tri-X, properly processed, would not lose ten percent density when stored at room temperature and 40 percent relative humidity for 100 years.³⁸ Thus, it must be concluded that any advantage Agfapan Vario-XL offers in terms such as speed-to-grain, exposure latitude, or silver recovery must be weighed carefully against the reduction in image stability of the film negative material.

LIST OF REFERENCES

LIST OF REFERENCES

1. R. J. Tuite, "Image Stability in Color Photography," Journal of Applied Photographic Engineering, 5, 200 (1979).
2. G. Fisher-Taylor, "Interview: Henry Wilhelm," Photo-Communique, 3, 5 (1981).
3. L. H. Feldman, "Discoloration of Black-And-White Photographic Prints," Journal of Applied Photographic Engineering, 7, 1 (1981).
4. P. Z. Adelstein and L. L. McCrea, "Dark Image Stability of Diazo Films," Journal of Applied Photographic Engineering, 3, 173 (1977).
5. B. Schwalberg, "First Look--Agfapan Vario-XL," Popular Photography, 87, 102-105 (1980).
6. L. A. Mannheim, "Best Film Ever? Ilford XP1," Modern Photography, 44, 98-101 (1981).
7. D. O'Neill, "Agfa Vario XL Vs Ilford XP1," Camera 35, 26, 56-59, 72-73 (1981).
8. D. C. Hubbell, R. G. McKinney, and L. E. West, "Methods for Testing Image Stability of Color Photographic Products," Photographic Science and Engineering, 11, 295-305 (1967).
9. Method for Comparing the Color Stabilities of Photographs, American National Standards Institute PH 1.42-1 (1969).
10. Ibid.
11. Hubbell, et. al., p. 296.
12. Tuite, p. 200.
13. C. C. Bard, G. W. Larson, H. Hammond, and C. Packard, "Predicting Long-Term Dark Storage Dye Stability Characteristics of Color Photographic Products from Short-Term Tests," Journal of Applied Photographic Engineering, 6, 42 (1980).
14. Ibid.
15. Tuite, p. 201.

16. Bard, et. al., p. 43.
17. Spectral Diffuse Densities of Three-Component Subtractive Color Films, American National Standards Institute PH 2.1-1952 (R1969), p. 7.
18. Agfa-Gevaert Technical Bulletin, "Agfapan Vario-XL Professional Film," Dec. 16, 1980.
19. Bard, et. al., p. 43.
20. A. D. Rickmers and H. N. Todd, Statistics, An Introduction, McGraw-Hill Book Company, New York, 1967, p. 133.
21. Tuite, p. 201.
22. H. Wilhelm, Personal Communication, March 23, 1981.
23. T. Woodlief (ed), SPSE Handbook of Photographic Science and Engineering, John Wiley and Sons, Inc., New York, 1973, p. 836.
24. Ibid.
25. Rickmers and Todd, pp. 154-178.
26. Ibid, pp. 179-197.
27. Ibid, p. 220.
28. F. H. Steiger, "The Arrhenius Equation in Accelerated Aging Studies," American Dyestuff Reporter, 47, 287-290 (1958).
29. F. Daniels and R. A. Alberty, Physical Chemistry, Third Edition, John Wiley and Sons, Inc., New York, 1967, p. 326.
30. Ibid.
31. W. C. Gardiner, Jr., Rates and Mechanisms of Chemical Reactions, W. A. Benjamin, Inc., Menlo Park, Ca., 1969, pp. 24-37.
32. G. W. Castellan, Physical Chemistry, Addison-Wesley Publishing Co., Reading, Ma., 1964, pp. 600-608.

33. Y. Seoka, S. Kubodera, T. Aono, and M. Hirano, "Some Problems in the Evaluation of Color Image Stability," Journal of Applied Photographic Engineering, 8, 80 (1982).
34. S. E. Shepard, R. C. Houck, and C. Dittmar, "The Structure of Gelatin Sols and Gels," Journal of Physical Chemistry, 44, 185-207 (1940).
35. E. Bradbury and C. Martin, "The Effect of the Temperature of Preparation on the Mechanical Properties and Structure of Gelatin Films," Proceedings of the Royal Society, 214, 183-187 (1952).
36. Kodak Current Information Summary 50, "Evaluating Dye Stability of Kodak Color Products," January, 1980.
37. Fisher-Taylor, p. 17.
38. W. Lee, Eastman Kodak Company, Photographic Technology Division, Image Stability Section, Personal Communication, March 18, 1982.
39. D. S. Carr and B. L. Harris, "Solutions for Maintaining Constant Relative Humidity," Industrial and Engineering Chemistry, 14, 2015 (1949).
40. Ibid.
41. Ibid.
42. International Critical Tables, Vol. I, p. 68, Vol. III, pp. 211-212, McGraw-Hill Book Co., New York, 1926.
43. C. H. Giles, S. D. Forrester, R. Haslam, and R. Horn, "Light Fastness Evaluation of Colour Photographs," Journal of Photographic Science, 21, 20 (1973).
44. W. C. Jung, I. C. Timer Cookbook, Howard W. Sams and Co., Inc., Indianapolis, 1977, pp. 131, 162.
45. Kodak Publication B-3, "Kodak Filters for Scientific and Technical Uses," 1978, p. 56.
46. Unpublished Data Sheets, Eastman Kodak Company, Paper Service Division, August 1978.

APPENDICES

APPENDIX A.

Solutions for Maintaining Constant Relative Humidity

The following temperature/relative humidity relationships were interpolated using a Texas Instruments linear/non-linear regression analysis program and a TI-58C calculator.

<u>Temperature °C</u>	<u>Relative Humidity %</u>	<u>Regression Model</u>
Potassium Chloride, KCl ³⁹		
68	80.1	RH = -0.07 t + 84.84 r = 0.985
77	79.5	
85	78.9	
93	78.3	
Potassium Fluoride, KF ⁴⁰		
68	21.8	RH = 0.078 t + 16.46 r = 0.996
77	22.5	
85	23.1	
93	23.7	
Potassium Iodide, KI ⁴¹		
68	62.3	RH = 107.96 t ^{-0.1305} r = 0.994
77	61.2	
85	60.5	
93	59.7	
Potassium Carbonate, K ₂ CO ₃ ^{42,43}		
25-?	43-45	

APPENDIX B.

Spectral Data and TI 58C/59 Program for Calculating Printing Density.

<u>Wavelength</u>	<u>E_λ¹</u>	<u>S_λ²</u>	<u>O_λ³</u>	<u>E_λS_λO_λ</u>
380	12	100	.001	1.2
390	15	100	.008	12
400	18	95.5	.0154	26.5
410	21	87	.080	146
420	24	79	.145	275
430	28	69	.291	562
440	32	58	.293	544
450	37	46	.294	500
460	42	33	.296	410
470	47	22	.298	308
480	52	13.5	.300	211
490	57	7.1	.301	122
500	63	2.8	.303	53.4
510	69	.65	.305	13.7
520	75	.15	.307	3.45
530	81	.0035	.308	.873
540	87	.001	.310	.0270

$$D_p = -\log_{10} \frac{\int E_{\lambda} S_{\lambda} O_{\lambda} T_{\lambda} d\lambda}{\int E_{\lambda} S_{\lambda} O_{\lambda} d\lambda}$$

APPENDIX B. (continued)

TI Program

2nd Lbl A	X
Sto 1	Rcl 2
R/S	=
2nd Lbl B	Sum 4
Sto 2	Rcl 3
R/S	÷
2nd Lbl C	Rcl 4
Rcl 1	=
=	Log
Sum 3	R/S
Clr	2nd Lbl D
Rcl 1	CMs
	Clr
	R/S

A	-Enter ESO for
---	----------------

B	-Enter T
---	----------

C	→Calculates D_p
---	-------------------

D	-Clears
---	---------

Repeat for each wavelength of interest. (Generally 390nm - 490nm.)

APPENDIX C.

Calibration of Source for Light Stability Tests

During the course of experimentation it was discovered, much to the experimenter's chagrin, that the intensity and distribution temperatures of the GE 150 watt PH212 lamps varied from lamp to lamp and changed with lamp age. Thus, each lamp was calibrated to assure the same intensity and distribution temperature at the beginning of each light stability test. These parameters were also checked at the end of each experiment to ensure that there was not a significant difference in lamp aging from test to test.

The intensity and distribution temperature measurements were obtained with an EG&G Model 550-1 radiometer/monochromator/filter wheel system and a spectral computer program developed by Professor John Carson.

The output flux from each lamp was measured at 50 nm increments from 450 to 750 nm at regulated voltage settings of 100, 110, 120, and 130 volts. The spectral power data was converted to distribution temperatures and intensity for each lamp using Professor Carson's program. A Texas Instruments regression analysis program was used to determine the relationship between voltage, V , distribution temperature,

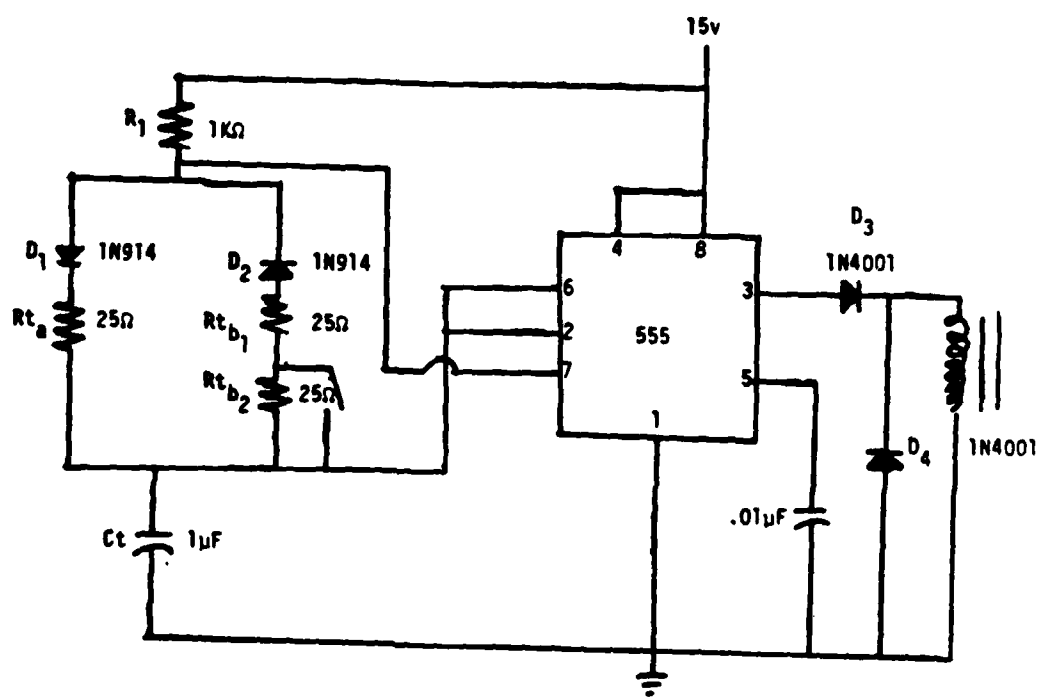
APPENDIX C. (continued)

DT, and illumination, E. It was found that $V = a_1 + a_2 DT^2$ and $V = a_3 E + a_4$ where a_1 , a_2 , a_3 , and a_4 are constants. The voltage was then calculated to yield a specific distribution temperature and illumination (3100 K and 472 footcandles). A twin variac rheostat and line voltage regulator were used to adjust and regulate the voltage.

It was also discovered that distribution temperature and illumination decrease with lamp age. Thus, replicate experiments were conducted using lamps with similar ages.

APPENDIX D.

Intervalometer Schematic



$$\text{On-time} = t_1 \approx 0.76 R_{t_a} C_t \approx 20 \text{ sec}$$

$$\text{Off-time} = t_2 \approx 0.76 R_{t_b} C_t \approx 40 \text{ sec}$$

$$t_1 \approx 20 \text{ sec (17 sec actual)}$$

$$t_2 \approx 40 \text{ sec (56 sec actual)}$$

Adapted from IC Timer Cookbook, W.C. Jung⁴⁴

APPENDIX E.

Average Transmittance Values Measured at 680 nm (Cyan) for Dark
Fading Conditions

FADE TIME (days)	TEMPERATURE (°C)											
	68°			77°			85°			93°		
	20%	45%	60%	80%	20%	45%	60%	80%	20%	45%	60%	80%
0	.125	.122	.124	.126	.124	.130	.129	.141	.113	.111	.108	.111
2	.137	.140	.145	.146	.152	.165	.180	.210	.185	.209	.202	.226
7	.170	.178	.190	.184	.224	.252	.277	.284	.311	.339	.331	.408
14	.205	.212	.212	.215	.337	.344	.4105	.471	.426	.445	.456	.590
21	.235	.231	.275	.423	.407	.536	.645	.507	.530	.592	.730	.697
28	.273	.271	.258	.328	.488	.474	-	-	-	-	-	-
35	.303	.293	.292	.381	.510	.513	-	-	-	-	-	-

APPENDIX F.

Analysis of Variance (ANOVA) Calculations.

1. Replicate Values used in Analysis ΔI (680nm):

		TEMPERATURE (°C)															
		68°C				77°C				85°C				93°C			
		RH				RH				RH				RH			
		20	45	60	80	20	45	60	80	20	45	60	80	20	45	60	80
DAY 7		.049	.058	.065	.065	.100	.122	.140	.139	.195	.230	.204	.263	.325	.327	.428	.554
		.042	.065	.066	.062	.101	.123	.137	.150	.201	.226	.203	.331	.343	.350	.435	.574
DAY 14		.084	.091	.087	.102	.212	.218	.303	.326	.316	.335	.349	.439	.489	.534	.639	.713
		.077	.089	.088	.099	.215	.210	.272	.313	.311	.332	.353	.518	.498	.542	.642	.729
DAY 21		.117	.117	.105	.156	.298	.284	.426	.500	.398	.423	.478	.608	.574	.634	.700	.857
		.104	.116	.109	.143	.301	.270	.409	.506	.389	.415	.483	.630	.582	.638	.698	.870

2. Mathematical Model:

$$\begin{aligned}
 X_{ijkl} = & \mu + T_i + RH_j + t_k + (T \times RH)_{ij} \\
 & + (RH \times t)_{jk} + (T \times t)_{ik} \\
 & + (T \times RH \times t)_{ijk} + \epsilon_{l(ijk)}
 \end{aligned}$$

where μ = Population mean

T_i = Temperature (°C) (Random)

RH_j = Relative Humidity (Random)

t_k = Time (days) (Random)

ϵ = Error

APPENDIX F (Cont)

3. Hypothesis:

$$H_0: \sigma_T^2 = 0, \sigma_{RH}^2 = 0, \sigma_t^2 = 0$$

4. Table of ANOVA Intermediate Values:

SOURCE	SUM OF SQUARES	v	MEAN SQUARE
Temp	2.92725	3	0.97575
RH	0.27213	3	0.090709
Time	0.70389	2	0.35195
Temp X RH	0.10404	9	0.011560
Temp X Time	0.11938	6	0.019896
RH X Time	0.02403	6	0.0040059
Temp X RH X Time	0.019706	18	0.0010948
Error	0.008129	48	0.00016935
TOTAL	4.178555	95	-

APPENDIX G.

Univariate Equations for Dark Fading.

Constant Values		$\Delta T = f(\text{temp})$	R^2	S.E.
Day 7, 20% RH	=	$1.57 - 0.0475T + 3.69 \times 10^{-4} T^2$	1.000	0.0003
Day 7, 45% RH	=	$0.762 - 0.0266T + 2.39 \times 10^{-4} T^2$	0.999	0.00068
Day 7, 60% RH	=	$2.66 - 0.0759T + 5.58 \times 10^{-4} T^2$	0.973	0.0447
Day 7, 80% RH	=	$3.26 - 0.0960T + 7.21 \times 10^{-4} T^2$	0.999	0.0091
Day 14, 20% RH	=	$0.386 - 0.0195T + 2.21 \times 10^{-4} T^2$	0.994	0.0225
Day 14, 45% RH	=	$1.07 - 0.0377T + 3.44 \times 10^{-4} T^2$	0.997	0.0176
Day 14, 60% RH	=	$1.26 - 0.0447T + 4.07 \times 10^{-4} T^2$	0.962	0.0770
Day 14, 80% RH	=	$-1.04 + 0.0109T + 8.51 \times 10^{-4} T^2$	0.994	0.0366
Day 21, 20% RH	=	$-0.857 + 0.0116T + 3.99 \times 10^{-5} T^2$	0.988	0.0374
Day 21, 45% RH	=	$0.436 - 0.0230T + 2.70 \times 10^{-4} T^2$	0.998	0.0178
Day 21, 60% RH	=	$-2.911 + 0.0608T - 2.39 \times 10^{-4} T^2$	0.969	0.0748
Day 21, 80% RH	=	$-10.2 + 0.253T - 1.47 \times 10^{-3} T^2$	1.000	0.000

f e

APPENDIX G. (continued)

<u>Constant Values</u>	<u>$\Delta T = f(RH)$</u>	<u>R^2</u>	<u>S.E.</u>
Day 7, 68°C	= 0.0245 +1.21 x 10 ³ RH -9.70 x 10 ⁻⁶ RH ²	0.904	0.0045
Day 7, 77°C	= 0.0616 +2.11 x 10 ³ RH -1.33 x 10 ⁻⁵ RH ²	0.919	0.0108
Day 7, 85°C	= 0.238 -2.53 x 10 ⁻³ RH +3.97 x 10 ⁻⁵ RH ²	0.791	0.0360
Day 7, 93°C	= 0.409 -5.12 x 10 ⁻³ RH +8.87 x 10 ⁻⁵ RH ²	0.993	0.0147
Day 14, 68°C	= 0.0714 +5.63 x 10 ⁻⁴ RH -4.31 x 10 ⁻⁶ RH ²	0.840	0.0030
Day 14, 77°C	= 0.226 -1.55 x 10 ⁻³ RH +3.64 x 10 ⁻⁵ RH ²	0.939	0.0244
Day 14, 85°C	= 0.380 -4.59 x 10 ⁻³ RH +7.21 x 10 ⁻⁵ RH ²	0.969	0.0228
Day 14, 93°C	= 0.467 +4.14 x 10 ⁻⁴ RH +3.55 x 10 ⁻⁵ RH ²	0.972	0.0295
Day 21, 68°C	= 0.137 -1.68 x 10 ⁻³ RH +2.24 x 10 ⁻⁵ RH ²	0.818	0.0144
Day 21, 77°C	= 0.356 -4.90 x 10 ⁻³ RH +8.60 x 10 ⁻⁵ RH ²	0.926	0.0493
Day 21, 85°C	= 0.442 -3.97 x 10 ⁻³ RH +7.73 x 10 ⁻⁵ RH ²	0.999	0.0013
Day 21, 93°C	= 0.553 +6.33 x 10 ⁻⁴ RH +2.88 x 10 ⁻⁵ RH ²	0.999	0.0059

APPENDIX G. (continued)

Constant Values	$\Delta T = f(\text{time})$	R^2	S.E.
68°C, 20% RH	= $0.123 + 5.76 \times 10^{-3}t - 1.92 \times 10^{-5}t^2$	0.994	0.0046
68°C, 45% RH	= $0.124 + 7.48 \times 10^{-3}t - 8.98 \times 10^{-5}t^2$	0.992	0.0051
68°C, 60% RH	= $2.21 \times 10^{-3} + 9.81 \times 10^{-3}t - 2.34 \times 10^{-4}t^2$	0.990	0.0065
68°C, 80% RH	= $4.51 \times 10^{-3} + 6.54 \times 10^{-3}t + 1.09 \times 10^{-5}t^2$	0.988	0.0092
77°C, 20% RH	= $-2.61 \times 10^{-3} + 0.0160t - 7.21 \times 10^{-5}t^2$	0.999	0.0064
77°C, 45% RH	= $3.90 \times 10^{-3} + 0.0189t - 2.80 \times 10^{-4}t^2$	0.998	0.0072
77°C, 60% RH	= $3.63 \times 10^{-3} + 0.022t - 1.11 \times 10^{-4}t^2$	0.999	0.0044
77°C, 80% RH	= $9.83 \times 10^{-3} + 0.020t - 1.802 \times 10^{-4}t^2$	0.996	0.0189
85°C, 20% RH	= $7.19 \times 10^{-3} + 0.0309t - 6.00 \times 10^{-4}t^2$	0.998	0.0077
85°C, 45% RH	= $0.0200 + 0.0342t - 7.43 \times 10^{-4}t^2$	0.990	0.0204
85°C, 60% RH	= $0.0196 + 0.0292t - 3.50 \times 10^{-4}t^2$	0.993	0.0184
85°C, 80% RH	= $0.0141 + 0.0451t - 7.86 \times 10^{-4}t^2$	0.998	0.0143
93°C, 20% RH	= $0.0105 + 0.0551t - 1.35 \times 10^{-3}t^2$	0.996	0.0190
93°C, 45% RH	= $0.0228 + 0.0561t - 1.29 \times 10^{-3}t^2$	0.995	0.0228
93°C, 60% RH	= $0.0194 + 0.0721t - 1.91 \times 10^{-3}t^2$	0.997	0.0184
93°C, 80% RH	= $0.0172 + 0.111t - 4.38 \times 10^{-3}t^2$	0.996	0.0252

APPENDIX H.

Bivariate Equations for Dark Fading

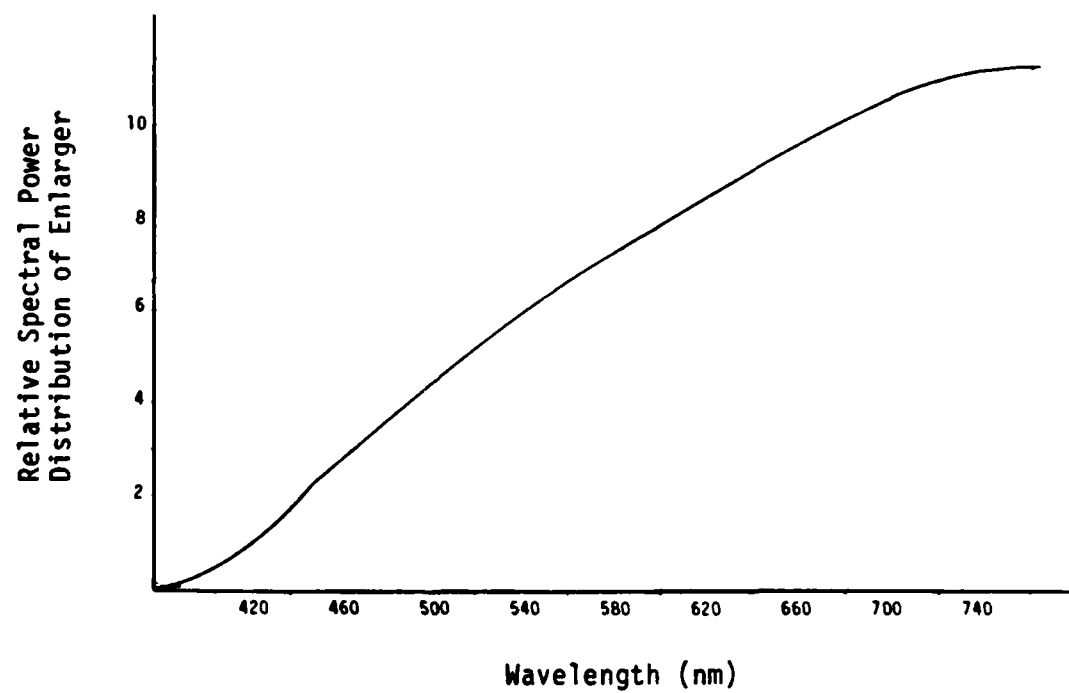
<u>Constant Value</u>	<u>$\Delta I = f(RH, \text{ time})$</u>	<u>R^2</u>	<u>S.E.</u>
68°C	$= 5.55 \times 10^{-3} + 6.88 \times 10^{-3}t - 2.05 \times 10^{-4} RH$ $- 1.14 \times 10^{-4}t^2 + 2.11 \times 10^{-6} RH^2 + 2.19 t RH$	0.972	0.0096
77°C	$= 0.0634 + 0.0106t - 2.91 \times 10^{-3} RH$ $- 8.30 \times 10^{-5}t^2 + 2.73 \times 10^{-5} RH^2 + 1.74 \times 10^{-4} t RH$	0.978	0.0278
85°C	$= 0.0930 + 0.0265t - 4.61 \times 10^{-3} RH$ $- 6.19 \times 10^{-4}t^2 + 4.73 \times 10^{-5} RH^2 + 1.75 \times 10^{-4} t RH$	0.990	0.0234
93°C	$= 0.0438 + 0.0583t - 3.37 \times 10^{-3} RH$ $- 1.71 \times 10^{-3}t^2 + 4.44 \times 10^{-5} RH^2 + 1.88 \times 10^{-4} t RH$	0.983	0.0438
<u>$\Delta I = f(\text{temp}, \text{ Time})$</u>			
20% RH	$= 0.785 - 0.226T - 0.0402t + 1.58 \times 10^{-4} T^2$ $- 5.19 \times 10^{-4}t^2 + 8.34 \times 10^{-4} T t$	0.976	0.0359
45% RH	$= 1.17 - 0.0319T - 0.0475t + 2.13 \times 10^{-4} T^2$ $- 6.16 \times 10^{-4}t^2 + 9.59 \times 10^{-4} T t$	0.984	0.0307
60% RH	$= 0.909 - 0.0261T - 0.0519t + 1.81 \times 10^{-4} T^2$ $- 6.50 \times 10^{-4}t^2 + 1.06 \times 10^{-3} T t$	0.958	0.0587
80% RH	$= 1.24 - 0.0353T - 0.0790t + 2.44 \times 10^{-4} T^2$ $- 5.24 \times 10^{-4}t^2 + 1.44 \times 10^{-3} T t$	0.953	0.0689

APPENDIX H. (continued)

<u>Constant Value</u>	<u>$\Delta T = f(\text{Temp, RH})$</u>	<u>R^2</u>	<u>S.E.</u>
Day 7	$= 2.57 - 0.0682T - 0.0116 \text{ RH} + 4.72 \times 10^{-4} T^2$ $+ 2.64 \times 10^{-5} \text{ RH}^2 + 1.30 \times 10^{-4} T \text{ RH}$	0.0974	0.0299
Day 14	$= 0.972 - 0.0301T - 0.0129 \text{ RH} + 2.64 \times 10^{-4} T^2$ $+ 3.49 \times 10^{-5} \text{ RH}^2 + 1.44 \times 10^{-4} T \text{ RH}$	0.983	0.0324
Day 21	$= 1.34 + 0.0280T - 0.0143 \text{ RH} - 8.24 \times 10^{-5} T^2$ $+ 6.20 \times 10^{-5} \text{ RH}^2 + 1.38 \times 10^{-4} T \text{ RH}$	0.969	0.0448

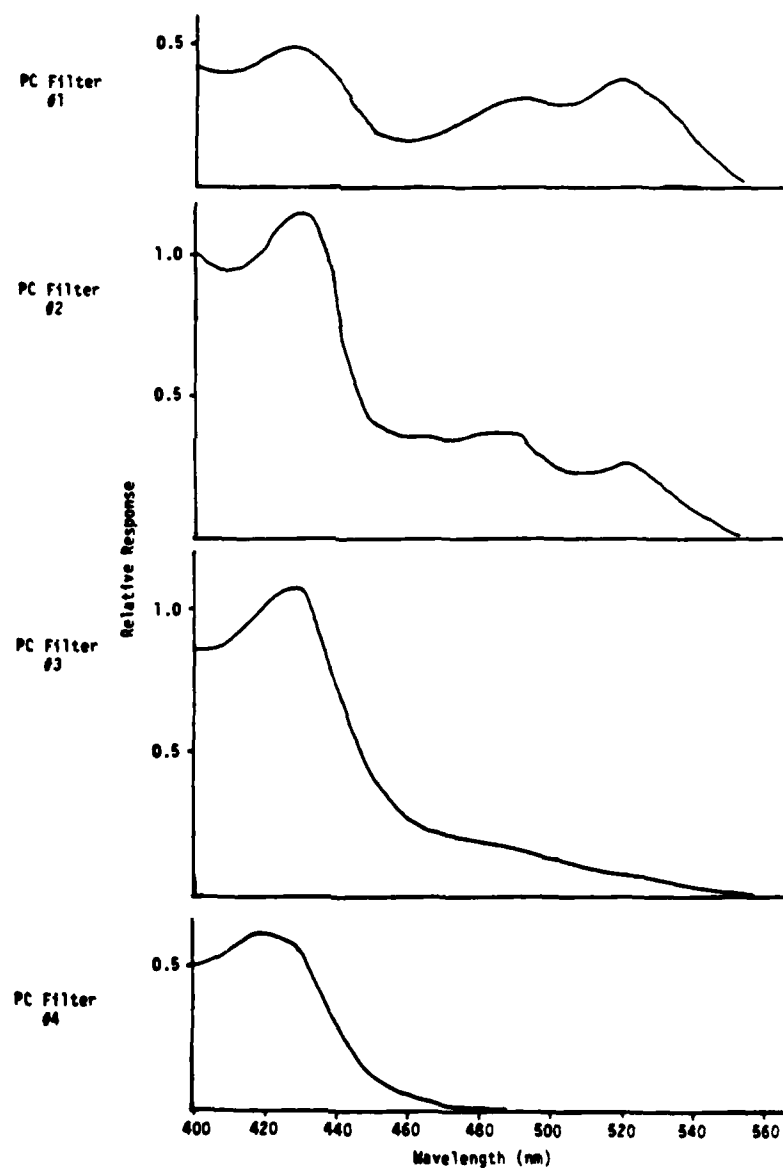
APPENDIX I.

Relative Power Distribution of Enlarger
(Combination of Lamp and Condenser)



APPENDIX J.

Product of Polycontrast Filter Response⁴⁵ and Spectral Sensitivity of Kodak Polycontrast Rapid II RC Paper Sensitivity⁴⁶.



VITA

VITA

C. P. Datema is an Air Force officer attending Rochester Institute of Technology under the Sponsorship of the Air Force Institute of Technology.

A Colorado native (born in Glenwood Springs, Colorado, December 18, 1945), he received his Bachelors Degree in chemistry from Bob Jones University in 1968 and an MBA from the University of Utah in 1974. He is also a graduate of Air Command and Staff College.

His military duties have included such varied assignments as an agreements and negotiations officer in Europe; a commander in Alaska; a management evaluator, inspecting Air Force organizations worldwide; and a tactical communications-electronics maintenance officer. His most recent assignment was with the Eastman Kodak Company, Photographic Technology Division, participating in the Air Force Education with Industry Program.